



HAL
open science

Main factors favoring *Mnemiopsis leidyi* individuals growth and population outbreaks: A modelling approach

Elena Alekseenko, M. Baklouti, F Carlotti

► To cite this version:

Elena Alekseenko, M. Baklouti, F Carlotti. Main factors favoring *Mnemiopsis leidyi* individuals growth and population outbreaks: A modelling approach. *Journal of Marine Systems*, 2019, 196, pp.14-35. 10.1016/j.jmarsys.2019.01.001 . hal-02184790

HAL Id: hal-02184790

<https://hal.science/hal-02184790>

Submitted on 17 Jul 2019

HAL is a multi-disciplinary open access archive for the deposit and dissemination of scientific research documents, whether they are published or not. The documents may come from teaching and research institutions in France or abroad, or from public or private research centers.

L'archive ouverte pluridisciplinaire **HAL**, est destinée au dépôt et à la diffusion de documents scientifiques de niveau recherche, publiés ou non, émanant des établissements d'enseignement et de recherche français ou étrangers, des laboratoires publics ou privés.

1 Main factors favoring *Mnemiopsis leidyi* individuals 2 growth and population outbreaks : a modelling approach

3 E. Alekseenko^{a,b,c,*}, M. Baklouti^a, F. Carlotti^a

4 ^a*Aix-Marseille Université, Université de Toulon, CNRS/INSU, IRD, MIO, UM 110,*
5 *13288, Marseille, Cedex 09, France*

6 ^b*P.P. Shirshov Institute of Oceanology, Russian Academy of Sciences, Nakhimovsky*
7 *Prospekt 36, 117997, Moscow, Russia*

8 ^c*Laboratoire des Sciences du Climat et de l'Environnement (LSCE/IPSL), CEA Saclay,*
9 *Gif-sur-Yvette, 91191, France*

10 **Abstract**

11 A population model of the marine invasive ctenophore species *Mnemiopsis*
12 *leidyi* (ML) including physiological and demographic processes has been in-
13 cluded in the flexible-stoichiometry biogeochemical marine ecosystem model
14 (Eco3M-MED). This model is used in order to define through several numeri-
15 cal simulations possible environmental windows favorable to ML adaptation
16 and outbreaks in invaded habitats, such as the coastal areas of the Medi-
17 terranean Sea. One of the strengths of the ML model is that it delivers the
18 functional response either expressed in terms of consumed individual prey or
19 in prey biomass, however the prey are expressed, as individual abundance
20 or biomass concentration. Numerical experiments were performed to test the
21 functional response in various quantitative and qualitative diet conditions.
22 Longer term experiments including starvation regimes were run to characte-
23 rize the response of the ML population in terms of growth rate and dynamics.

24 Our results firstly show that the required food conditions for ML out-
25 bursts, which involve combinations of food quality and quantity, should
26 mainly be found in the most productive Mediterranean coastal areas, and
27 more rarely in the open sea, and that variations in food concentrations may
28 induce rapid outbursts or collapse of ML populations. Results also indicate
29 that food concentrations directly impact reproduction, and that for a given
30 fixed available prey biomass, ML abundance is maximum for the prey of
31 richest nutritional value. As our model considers two levels of ecological in-
32 tegration, individual and population, it has been shown that the response to
33 starvation or to recovery from starvation after food replenishment occurs at

34 different time scales depending on the integration level.

35 Then, different scenarios of global change have been simulated in order
36 to analyze the inter-annual variability in ML population dynamics. Our mo-
37 del could reproduce typical 3 months ML blooms, which is also observed in
38 nature, and it suggests that this is the result of a combination of species
39 properties and environmental forcings. Our simulations also reveal that an
40 increase in temperature promotes the occurrence of jellyfish outbreaks. Fi-
41 nally, the strongest forcing influence on ML dynamics is the reduction of
42 fish competitors for food due to an increase in fishing pressure. This forcing
43 significantly impacts not only the frequency of the outbreaks, but also ML
44 accumulated population growth over a ten-year period. Finally, our simula-
45 tions call for long-term (over at least a ten-year period) observations with a
46 temporal resolution of one month or less.

47 *Keywords:* *Mnemiopsis leidyi*, mechanistic biogeochemical model Eco3M,
48 flexible-stoichiometry, prey quality, environmental window for ML
49 outbursts;

50 1. Introduction

51 The introduction of invasive aquatic species into new habitats has been
52 identified as one of the four greatest threats for the world oceans (Werschkun
53 et al, 2014). Aquatic invasions are virtually irreversible and, once the new-
54 comers are established, their impact may also increase in severity over time.
55 During the last decades, a dramatic increase in the number of alien species
56 has been observed in different marine ecosystems. Many of these species be-
57 came successfully adapted to their new habitats, thereby leading to serious
58 ecosystem changes, disruptions of ecosystem services and the associated eco-
59 nomic consequences (Vila et al., 2010). The transfer of invasive species does
60 not only occur over larger distances, between continents, but also locally,
61 over regional seas (David et al., 2013).

62 One recent example of a drastically impacting invasive species is the ge-
63 latinous zooplankton – ctenophora *Mnemiopsis leidyi*, referred to as ML he-
64 reafter (Pitt & Lucas, 2013). The species ML originates from the east coast
65 of the USA and the Caribbean Sea and was introduced in the early 1980s in
66 the Black Sea and the Azov Sea, where it could spread, and sometimes domi-
67 nate the local food webs due to its high adaptation capacity in combination
68 with increasing shipping traffic, global warming, eutrophication, pollution

69 and overfishing. This led to a devastating reduction in fish catch levels in
70 these seas (Shiganova & Bulgakova, 2000; Mills, 2001; Byers, 2002; Sali-
71 hoglu, 2011). Since then, ML has spread further and it is also found today
72 in a wide range of habitats in Eurasian seas : from the brackish closed and
73 semi-closed seas and lagoons to the Mediterranean Sea and Atlantic coastal
74 areas, from temperate to subtropical regions, from high productive to oligo-
75 trophic environments (Pitois & Shiganova, CIESM, 2015). ML is a highly
76 opportunistic species : a simultaneous hermaphrodite with direct develop-
77 ment, capable of self-fertilization; what means that viable offspring can be
78 produced from a single adult (Purcell et al., 2001). When food is abundant,
79 each organism can ingest up to ten times its own body weight during a single
80 day, which is far more than it is able to digest. Inversely, an organism can
81 survive for up to three weeks without food (Finenko et al, 2010). ML is found
82 in an extremely wide range of environmental conditions, from cold (0°C) to
83 warm (32°C) waters, with salinities ranging from <2 to 45‰ (Purcell et al,
84 2001, Pitt & Lucas, 2014, Kremer 1994, Colin et al, 2010, Shiganova et al,
85 2001, 2011). Consequently, ML presents a tremendous potential for growth,
86 survival and reproduction that enables this species to be a predominant zoo-
87 planktivore in a wide variety of habitats. Especially in estuarine and coastal
88 waters, ctenophores can reach very high abundance, since it feeds on prey
89 ranging from microplankton (50 microns) to fish larvae (> 3 mm) by clearing
90 large volumes of water (Colin et al. 2010).

91 The high number of ML recorded during the last years along the Medi-
92 terranean coastlines (Fig. 1), especially along the northern coast (Galil et
93 al., 2009; Boero et al., 2009; Fuentes et al., 2010; Kylie and Lucas, 2014),
94 strongly suggest that ML is now well established in the Mediterranean Sea.
95 From an ecosystem perspective, the apparent increase and synchrony in jel-
96 lyfish outbreaks in both the western and eastern Mediterranean basins are
97 sending warning signals of a potential phase shift from a fish to a "gelatinous
98 sea" (Boero, 2013).

99 Climate warming, eutrophication, coastal habitat degradation and over-
100 fishing are among the most probable drivers of ML development, though the
101 invasion pathways of this species and the reasons for its successful coloniza-
102 tion of new habitats are not well identified yet, and the lack of data makes
103 any further investigation difficult. The recent knowledge on the impact of cli-
104 mate warming, eutrophication, coastal habitat degradation and overfishing
105 on ML development has led to the following conclusion :

106 — Field observations of ML species revealed that its physiology is tempe-

107 rature dependent (Javidpour et al., 2009) and global warming is likely
108 to affect the timing and distribution of ML in those areas (Pitois &
109 Shiganova, CIESM, 2015).

110 — It was observed that ML was very abundant in coastal and lagoon
111 waters, which are highly affected by eutrophication. Eutrophication
112 has become a major component of coastal habitat degradation in the
113 Mediterranean during the last decades (MerMex group, 2011). Lud-
114 wig et al. (2009) report increasingly high loads of dissolved inorganic
115 nitrogen associated with an increase in the $NO_3 : PO_4$ ratio of the
116 Mediterranean river outputs. This ratio determines which nutrient
117 will limit biological productivity at the base of the food web and may
118 select plankton communities with distinct biogeochemical functions
119 (Deutsch & Weber, 2012).

120 — Overfishing may also play a crucial role in the development of ML.
121 One of the well-known cases is the Black Sea in 1989 where ML has
122 strongly developed by emptying the ecological niche occupied by small
123 pelagic fishes, thereby allowing gelatinous competitors to reinhabit
124 (Gucu, 2002).

125 Modelling can provide an additional understanding of mechanisms through
126 the characterization of environmental conditions that could support and/or
127 favor the gelatinous zooplankton ML and the description of the associated
128 changes in the planktonic community structure.

129 Several models describing ML behavior have already been used for various
130 specific studies. Among them are individual-growth models constructed by
131 Kremer (1976), Kremer & Reeve (1989) for the study of ML development
132 in Narragansett Bay. Salihoglu et al. (2011) and Shiganova et al. (2018)
133 have developed a zero-dimensional population-based model considering four
134 stages, namely : egg, juvenile, transitional and adult stages, and the asso-
135 ciated processes. In the two latter studies, the model used could represent
136 consistent development patterns in the Black Sea. All the above-mentioned
137 models offer a basis for the study of ML behavior within different size or age
138 classes. Food concentration and temperature were the main forcings consi-
139 dered in these models, which do not consider the other trophic levels of the
140 planktonic food web. Also, these 0D models are designed to simulate ML
141 dynamics in a given region of interest. Oguz et al. (2008) developed a model
142 including the lower trophic levels of the planktonic food web by considering
143 three phytoplankton groups, three zooplankton groups (as we do in our mo-
144 del), and a simplified particulate and dissolved nitrogen cycle. This model

145 was used in a two-layer configuration (i.e. the 0-50m euphotic zone and the
146 sub-thermocline layer) in the Black Sea.

147 Another group of models considers ML dynamics in a three-dimensional
148 configuration. Among them are statistical models based on the estimation
149 of the probability of ML occurrence, which depends on different key factors
150 measured in situ (Collingridge et al., 2014 and Siapatis et al., 2008). One of
151 these models is used to study the North Sea and Baltic Sea (Collingridge et
152 al., 2014), and the other, - the Aegean and Mediterranean seas (Siapatis et
153 al., 2008). The limits of the statistical approach lie in the fact that it does not
154 take into account the key processes of ML population growth, reproduction,
155 metabolic demands and mortality. Mechanistic three-dimensional models are
156 designed for this purpose. Van der Molen et al. (2015) and David et al. (2015)
157 have performed an extensive study using a multi-model approach with dif-
158 ferent types of models, namely a high-resolution particle tracking model with
159 passive particles, a low-resolution particle tracking model with a reproduc-
160 tion model coupled to a biogeochemical model, and a dynamic energy budget
161 (DEB) model. The aim of these works was to investigate the reasons for t
162 ML dispersal in the region of the Scheldt estuaries and the southern North
163 Sea. Analysis of the influence of temperature and food variability on ML
164 reproduction and outbursts have been performed in these works.

165 We propose here another mechanistic model, based on the Eco3M-MED
166 biogeochemical model (Alekseenko et al., 2014), in which we have added a
167 new compartment for ML. This model has several advantages in that (i) it
168 considers seven plankton functional types (PFTs) from bacteria to ML, (ii)
169 C, N and P biogeochemical cycles are described in the model; (iii) organisms
170 are represented in terms of abundance (ind.l^{-1}) and in terms of C, N and P
171 concentrations (mol.l^{-1}), thereby offering the possibility to handle intracel-
172 lular ratios and also intracellular quotas that influence the kinetics of most
173 of the physiological processes undertaken by each PFT.

174 The aim of this paper is to investigate through a theoretical study, the
175 impact of several external factors (namely temperature, food availability and
176 quality (stoichiometry)) on ML physiology and population dynamics and to
177 define environmental windows leading to ML blooms. Though theoretical,
178 this study also aims at providing “realistic” results, in the sense that they
179 could help in understanding some aspects of ML dynamics in the Mediterra-
180 nean Sea.

181 **2. Materials and methods**

182 *2.1. Terminology*

183 In this paper, the terms abundance and concentration will respectively
184 refer to a number of individuals per unit volume and to a C (or N, P) biomass
185 in mol per unit volume. Internal quota term (in mol.ind⁻¹) will correspond
186 to the X biomass per individual, and internal ratio (in molX.molY⁻¹ where
187 X and Y stand either for C, N or P) to the proportion of biomasses C :N,
188 C :P, N :P. Relative quotas (varying in the range 0-100 %, see eq. 1) will be
189 also be used in this work.

$$\widetilde{Q}_X = \frac{Q_X - Q_X^{min}}{Q_X^{max} - Q_X^{min}} \cdot 100\%. \quad (1)$$

190 *2.2. General features of Eco3M-MED model*

191 The Eco3M (Ecological Mechanistic and Modular) modelling tool (Bak-
192 louti et al. 2006a, b) is used in this work. Several configurations (i.e. several
193 flexible-stoichiometry models representing the low levels of the marine food
194 web) have already been embedded in this tool featuring a modular structure
195 (e.g., Baklouti et al. 2006b; 2011; Eisenhauer et al., 2009; Fontana et al.
196 2009; Auger et al. 2011, Alekseenko et al. 2014; Guyennon et al., 2015).

197 In a recent configuration of Eco3M (referred to as Eco3M-MED, Alek-
198 seenko et al., 2014; Guyennon et al., 2015), organisms are represented both
199 in terms of elemental concentrations (in mol C, N or P per liter) and abun-
200 dances (in cells or individuals per liter), thereby enabling the delivery of
201 internal quotas (in mol C, N or P per cells) in addition to internal ratios
202 (in mol X per mol Y). These internal quotas and ratios are calculated dy-
203 namically for each organism and contribute to the kinetics of regulation of
204 most of the physiological processes included in the model. The introduction
205 of abundances has several other advantages : it enables a direct comparison
206 (i.e., without using a conversion factor from biomasses, as is usually done)
207 of the model outputs with the growing data set of bacteria, phytoplankton
208 or zooplankton abundances that are provided by recent techniques such as
209 flow cytometry and plankton counts. It also makes it possible to differentiate
210 in the modeled population biomass growth the respective contributions of
211 organism recruitment (production of new organisms) and biomass synthesis.

212 The conceptual scheme of the biogeochemical model Eco3M-MED used
213 in this study accounts for the complex food-web of the NW Mediterranean

214 Sea (Fig. 2). Compared to the previous version of Eco3M-MED described in
 215 Alekseenko et al. (2014), a new functional type has been introduced in the
 216 planktonic food web, namely the gelatinous carnivorous zooplankton repre-
 217 sented by the species ML. Therefore, the Eco3M-MED model developed in
 218 this work includes the following 40 state variables :

- 219 — Three nutrients : nitrate (NO_3), phosphate (PO_4), and ammonium
 220 (NH_4). Silicate is not considered here since it is assumed that, in the
 221 Mediterranean Sea, it does not limit diatom growth.
- 222 — Dissolved organic matter (DOM) constituted by labile and semi-
 223 labile organic carbon ($LDOC$, $SLDOC$), labile organic phosphorus
 224 ($LDOP$), and labile organic nitrogen ($LDON$).
- 225 — Particulate organic detrital matter (POM) constituted by : carbon,
 226 phosphorus and nitrogen (POC , POP , PON).
- 227 — Bacterial cells with their carbon, nitrogen and phosphorus content
 228 (BAC , BAC_C , BAC_N , BAC_P).
- 229 — Two size classes of phytoplankton cells ($<10 \mu\text{m}$ and $>10 \mu\text{m}$; refer-
 230 red to as "small" and "large" in the model) with their carbon, nitro-
 231 gen, phosphorus and chlorophyll content ($PHYS$, $PHYS_C$, $PHYS_N$,
 232 $PHYS_P$, $PHYS_{Chl}$ and $PHYL$, $PHYL_C$, $PHYL_N$, $PHYL_P$, $PHYL_{Chl}$).
- 233 — Four compartments of zooplankton organisms with their carbon, ni-
 234 trogen, and phosphorus contents : nano-, micro-, meso- and gela-
 235 tinous zooplankton represented respectively by heterotrophic nano-
 236 flagellates (HNF , HNF_C , HNF_N , HNF_P), ciliates (CIL , CIL_C ,
 237 CIL_N , CIL_P), copepods (Z , Z_C , Z_N , Z_P) and ML (ML , ML_C , ML_N ,
 238 ML_P).

239 2.3. ML population model and terminology

240 ML adult life stage is explicitly represented in the model. ML adults are
 241 able to reproduce under certain conditions of their physiological state. The
 242 reproduction rate and most of the physiological processes undertaken by these
 243 adults are indeed regulated by their internal quotas of carbon, nitrogen and
 244 phosphorus (Q_C , Q_N and Q_P). The minimum and maximum quota values
 245 are given in Table 1.

246 The ML life phase between egg and adult stages, hereafter called the "ju-
 247 venile phase", is not explicitly represented. This phase actually includes both
 248 larval and juvenile individuals and lasts between 16 and 40 days depending
 249 on the food density and water temperature (Collingridge et al., 2014, Sali-
 250 hoglu et al., 2011). We also assume that juveniles have not yet reached the

251 minimum nutritional state necessary to achieve reproduction. Thus, recruited
252 adults from juveniles are not yet sexually mature and they will be referred to
253 as immature adults. T_{rep} stands for the time necessary for immature adults
254 to reach the mature stage for reproduction (i.e. the time to become mature
255 adults). For mature adults, as spawning occurs, the entire amount of mate-
256 rial required to grow from egg stage to adult stage is instantly and explicitly
257 transferred from the prey biomass pools (copepods and ciliates) to the ML
258 adult pool. In other words, the lag time between the egg and adult stages is
259 not accounted for by the model, but the accumulated ingested food needed
260 for the juvenile growth is explicitly taken into account through implicit ML
261 juvenile grazing on ML prey.

262 In the following sections, we will use the term specific population growth
263 rate (SPGR in h^{-1}) to express the number of new individuals per individual
264 and unit time. The population growth rate (PGR in $\text{ind.l}^{-1}.\text{h}^{-1}$) will refer
265 to the increase in the number of individuals per unit volume and unit time.
266 The specific growth rate (SGR in $\text{molC.molC}^{-1}.\text{h}^{-1}$ or in h^{-1}) to express the
267 biomass change of an individual per mean biomass and unit time.

268 2.4. *ML activities*

269 This section describes the model formulation of ML physiological and de-
270 mographic processes. The processes and the assumptions used to establish the
271 associated formulations are presented in a specific subsection. Fig. 3 shows
272 a schematic representation of ML physiological processes that have been in-
273 corporated in the Eco3M-MED biogeochemical model. Table 2 contains the
274 list of model functions.

275 2.4.1. *Feeding*

276 Dietary flexibility allows ML to exploit a wide range of planktonic food
277 sources, such as microplankton, mesozooplankton, and fish eggs (Costello
278 et al., 2012, Purcell et al., 1994, 2001), thereby revealing an essential trait
279 associated with the invasive success of ML.

280 A review of the nature of the prey ingested by ML is presented in Costello
281 et al. (2012, their Table 2), based on in situ gut content from various geo-
282 graphical locations, including ML native and invaded ecosystems. According
283 to this review, the dominant prey found in ML gut is copepod for most eco-
284 systems. In another survey, Purcell et al (2012) suggest that direct predation
285 on eggs and fish larvae appears to be of a secondary order compared to the

286 predation on zooplankton. Hamer et al. (2010) corroborate this by investi-
 287 gating the potential link between ML and fish populations, performing ML
 288 feeding experiments on both eggs and larvae. They found no significant cor-
 289 relation could be detected between ML abundance and the abundance of fish
 290 eggs. In the same study, C and N stable isotope signatures of three potential
 291 prey groups (fish eggs, small plankton and larger plankton) showed that ML
 292 primarily feeds on plankton, while fish eggs are of minor importance. In ad-
 293 dition, a feeding selection experiment, with fish eggs and copepods offered in
 294 the same proportion, corroborated these findings : ML ingested significantly
 295 more copepods, and feeding on fish eggs was not significantly different from
 296 zero. Finally, Hamer et al. (2010) showed that ML has no serious potential as
 297 a direct predator of fish eggs, but individuals of this species might compete
 298 for food with larval fish. In the Mediterranean and Black seas, the contribu-
 299 tion of ichthyoplankton to *M. leidyi* diet seems to be negligible according to
 300 a large number of studies (CIESM, 2011, Finenko et al., 2013). On the basis
 301 of these observations, ML prey were restricted to zooplankton in our model.

302 The abundance and composition of zooplanktonic prey are likely to in-
 303 fluence ML population dynamics differently depending on the life stage (Mc-
 304 Namara et al., 2013). Whereas laboratory measurements of ML clearance
 305 rates showed a preference of ML adults for copepods (Madsen & Riisgard,
 306 2010), ML juveniles exert significant predatory control over planktonic ci-
 307 liates and other microzooplanktonic compartments, including copepod *nau-*
 308 *plii* (Stoecker et al., 1987; Sullivan & Gifford, 2004, 2007). Despite the fact
 309 that only the ML adult stage is explicitly represented in the present version
 310 of the model, an implicit representation of the ML juvenile grazing impact
 311 on different food sources is included. That means that C, N and P quotas
 312 which are affected to each new adult organism in the model come from a
 313 small part (the egg weight) from their mother's C, N and P pool, but the
 314 rest come from the C, N and P pools of the ML juvenile's prey, namely co-
 315 pepods (arbitrarily representing 80 % of the food) and ciliates (20%). This
 316 implicit specific feeding rate during the juvenile stage is represented in the
 317 model through the function :

$$f^{gjuv} = \sigma Q_X^{min} f^\mu, \quad (2)$$

318 where Q_X^{min} is the minimum internal quota in element X for an ML adult,
 319 σ is the proportion of Q_X^{min} which is taken by ML from their preys during
 320 their implicit juvenile stages, f^μ is the function describing the specific rate

321 of ML growth (described in the next subsection).

322 The specific feeding rate of adult ML is represented by a Holling II for-
323 mulation revisited by Koojman (2010) :

$$f_{ML}^{gz} = \frac{I_m [Z]}{\frac{I_m}{F} + [Z]}, \quad (3)$$

324 where I_m is the maximum ingestion rate of ML, F the clearance rate, and
325 $[Z]$ the mesozooplankton abundance.

326 As already done in Baklouti et al. (2011), a feedback regulation of the
327 gross grazing flux is operated through the h^{Qx} quota function representing
328 the feedback of the internal individual status on ML feeding. The mathema-
329 tical expression of this quota function is given by Eq. (4) which has already
330 been used in Geider et al. (1998) to regulate net uptake of nutrient by phy-
331 toplankton :

$$h^{Qx} = \left(\frac{Q_X^{max} - Q_X}{Q_X^{max} - Q_X^{min}} \right)^{0.06}. \quad (4)$$

332 The excess of a given element X among C, N, and P goes to particulate
333 organic matter (*POM*).

334 2.4.2. Population growth and reproduction

335 The classical Droop formulation (Eq.5) combined with Leibig's law of the
336 minimum are used to describe the specific growth rate f^μ in the model :

$$f^\mu = \bar{\mu} \cdot \min_X \left[1 - \frac{Q_X^{min}}{Q_X} \right]. \quad (5)$$

337 In this formulation, Q_X represents the actual intracellular quota in a given
338 element X among C, N, and P, and $\bar{\mu}$ the maximum theoretical growth rate
339 of ML.

340 Q_X^{min} is the amount of element X used in ML organism structure and
341 metabolism and exceeding amount can be used as storage for growth and
342 reproduction. In the model, it is assumed that all ML adults, in which Q_X
343 exceeds Q_X^{min} , are mature (i.e. able to reproduce).

344 2.4.3. Mortality

345 The natural mortality specific rate f^m is represented through a kinetic
346 rate depending on the following relative carbon internal quota \widetilde{Q}_C :

$$f^m = \begin{cases} k_m, & \text{if } Q_C \geq Q_C^{min}, \\ k_m + A (2\widetilde{Q}_C)^2, & \text{if } Q_C < Q_C^{min} \text{ (i.e. } \widetilde{Q}_C < 0), \end{cases} \quad (6)$$

347 where k_m is the minimum specific mortality rate and A is a constant.

348 Equations (6) suggest that when ML adults have deficient nutritional
 349 states (i.e. $Q_C < Q_C^{min}$), their natural mortality rate is enhanced. In sub-
 350 stance, we assume that the specific natural mortality increases quadratically
 351 with \widetilde{Q}_C .

352 A quadratic mortality function is also applied to ML to implicitly re-
 353 present its predation by higher trophic levels :

$$f^{mq} = k_{mq}, \quad (7)$$

354 where k_{mq} is the specific quadratic mortality rate.

355 2.4.4. Metabolic requirements

356 In several models describing ML activities (Kremer & Reeve, 1989; Sali-
 357 hoglu et al., 2011), it is assumed that ML individual mass reduction is mainly
 358 due to respiration and to excretion losses exceeding assimilated inputs. Fur-
 359 thermore, laboratory experiments show a linear relationship between the ML
 360 respiration rate and food availability (Kremer 1982, Finenko et al. 1995, An-
 361 ninsky et al. 1998).

362 In the present model, ML respiration formulation is split into two terms :
 363 the first represents the energetic costs associated with the basal maintenance
 364 (which is related to carbon biomass), while the second term expresses the
 365 costs induced by the ingestion process (active metabolism).

$$f^{resp} = \begin{cases} r_m \cdot \left(1 + \frac{Q_C - Q_C^{min}}{Q_C}\right) + r_i \cdot f_{ML}^{gz}, & \text{if } Q_C \geq Q_C^{min} \\ r_m + r_i \cdot f_{ML}^{gz}, & \text{if } Q_C < Q_C^{min} \end{cases} \quad (8)$$

366 where r_m is the metabolic respiration-excretion rate and r_i the respiration
 367 cost due to ingestion requirements.

368 This formulation suggests that when the carbon reserve pool is not empty
 369 (i.e. $Q_C > Q_C^{min}$), the respiration associated with the individual maintenance
 370 is taken into account in addition to the basal respiration and to respiration
 371 costs for ingestion. The excretion formulation taken into account in the model
 372 is :

$$f_{excr}^X = f^{gz} Q_X^Z (1 - h^{Qx}) + r_m. \quad (9)$$

373 Only the equations relative to the new features of the model are presented
 374 here (Appendix A). The remaining equations can be found in Alekseenko et
 375 al. (2014).

376 3. Simulations and scenarios

377 Different modelling scenarios have been considered in this study (Table
 378 3) :

- 379 — TS1 : Analysis of the effective functional response and comparison
 380 with the theoretical one ; in this scenario, the level of ML adult's food
 381 (i.e. copepods) is set to constant ;
- 382 — TS2 : experiments on the impact of the diet quantity and quality on
 383 the time necessary for just-recruited ML to reach sexual maturity ;
 384 only ML immature adults are present at the beginning of the simula-
 385 tion ; in TS2a scenario, the impact of several food levels is investiga-
 386 ted while in TS2b, the quality of prey on the dynamics is investigated
 387 through simulations using different prey abundances corresponding
 388 to the same food concentration in terms of carbon biomass ; in TS2c
 389 scenario the impact of temperature and Q_{10} on SGR of mature and
 390 immature ML individual is investigated ;
- 391 — TS3 : Starvation experiments ; in this scenario, ML adults are starved
 392 for more or less long periods and then food is reintroduced at different
 393 fixed levels ;
- 394 — TS4 : 0D microcosm experiments ; in this scenario, the whole of the
 395 trophic web is explicitly represented and forced by dynamic light and
 396 temperature conditions ;
- 397 — TS5 : Nutrient ratio experiments ; this scenario investigates the impact
 398 of varying inorganic NO_3 and PO_4 concentrations and $NO_3 : PO_4$
 399 ratios ;
- 400 — TS6 : Competitive pressure on ML prey ; this scenario investigates the
 401 impact of different competition pressures exerted on ML prey, namely
 402 copepods.

403 In scenarios TS1 to TS3 , temperature is fixed while it varies according
 404 to the function plotted in Fig.10 (Q_{10} function) in the remaining scenarios.

405 In scenarios TS4 to TS6 , copepod abundance and biomass are not constant,
 406 but derived from the biogeochemical model forced by a light seasonal cycle

407 in the NW Mediterranean Sea. However, results will not be interpreted in
408 terms of seasonality but in terms of variation with time expressed in weeks
409 or years (for long-term simulations), since the seasonality of hydrodynamic
410 features cannot be reproduced with a 0D model.

411 3.1. *Effective functional response experiment (TS1)*

412 Scenario TS1 was designed to mimic ML-copepods laboratory experi-
413 ments in chemostat. It consisted in several numerical experiments in which
414 the abundance of ML's food (i.e. copepods) was set at a given value, while the
415 lower trophic levels were not considered. Eleven copepod abundance levels
416 ranging between 2.5 ind.l⁻¹ and 250 ind.l⁻¹ have been tested. The duration
417 of each simulation was 10 days. For these numerical experiments, copepods
418 were the only food source for ML juveniles and adults. Copepods were charac-
419 terized by a constant internal content in N and P equal to : $\widetilde{Q}_N = \widetilde{Q}_P = 50\%$
420 . In 9 experiments out of 11, copepods' relative internal carbon content was
421 set to 50%. Two experiments were run just for Z abundance of 250 ind.l⁻¹ in
422 which \widetilde{Q}_C was not equal to 50% : one using $\widetilde{Q}_C = 0\%$ and the other in which
423 $\widetilde{Q}_C = 100\%$.

424 3.2. *Impact of diet quality and quantity on ML growth (TS2)*

425 Scenario TS2a was performed to assess the necessary time for ML im-
426 mature adults to reach the nutritional status allowing their sexual maturity
427 (and thereby their reproduction) as a function of food availability (cope-
428 pods). For this, only ML immature adults (characterized by an internal quo-
429 tas $Q_C = \sigma Q_C^{min}$, $Q_N = \sigma Q_N^{min}$, $Q_P = \sigma Q_P^{min}$, which are listed in the Table
430 1) are introduced at the beginning of the simulation. Since σ is a proportion
431 of C, N and P taken by juvenile ML from its predators and it is below 1.
432 So, in this case \widetilde{Q}_C , \widetilde{Q}_N , \widetilde{Q}_P are below zero. They fed on copepods for which
433 abundance and internal quotas are set to constant ($\widetilde{Q}_N = \widetilde{Q}_P = 100\%$ and
434 $\widetilde{Q}_C = 50\%$, in order to simplify the interpretation of the experiment, N and
435 P are not limiting copepod growth). As for TS1, this scenario also mimics
436 chemostat-like laboratory experiments with copepod abundance set at the
437 desired level during the experiment.

438 Several abundances of copepod were used : 2.5, 5, 10, 25, 100 and 250
439 ind.l⁻¹. As for scenario TS1 , food abundance and biomass were maintained
440 constant during the whole of the simulated period. The duration of each
441 simulation equals 12 weeks.

442 TS2b is a complimentary scenario, which is analogous to TS2a, but the
443 duration of this scenario is much longer (1 year), and the number of tested
444 copepod abundances is limited to three values. The main idea of such a
445 scenario is to study the impact of food quality (for a given food quantity)
446 on ML dynamics. The food quantity (i.e. copepod biomass) is set to $7.5 \cdot$
447 $10^{-5} \text{ molC.l}^{-1}$, corresponding to three different combinations of the copepod
448 abundance and internal carbon content : (a) 250 ind.l^{-1} with $\widetilde{Q}_C=0\%$, (b)
449 150 ind.l^{-1} with $\widetilde{Q}_C=50\%$, and (c) $107.14 \text{ ind.l}^{-1}$ with $\widetilde{Q}_C=100\%$.

450 Another complementary scenario TS2c has been performed in order to in-
451 vestigate the impact of temperature on individual specific growth rate (SGR)
452 of mature (adult, able to reproduce) and immature (juvenile, unable to re-
453 produce) ML. This scenario was designed so as to reproduce laboratory ex-
454 periments. The goal was to compare modeled SGR values with laboratory
455 measurements available in literature. It is worth noting that the laboratory
456 experiments on ML's SGR were held under different temperature conditions.
457 For a better comparison with the different available data, four levels of im-
458 posed constant copepod abundance (20, 50, 100 and 200 ind.l^{-1} , the same
459 numbers as in Reeve et al., 1989 and in Purcell et al., 2001) with $\widetilde{Q}_C=100\%$
460 have been given to a juvenile ML under different temperature conditions (11,
461 14, 20 and $26 \text{ }^\circ\text{C}$).

462 Another important temperature-related parameter which impacts SGR
463 values is Q_{10} . For all experiments in this work, the Q_{10} of 1.5 has been taken
464 from Salihoglu et al. (2013), for ML in the Black Sea. However other observa-
465 tions from the native environment showed that Q_{10} was varying, depending
466 on ML biomass (Kremer, 1979, typically from 1.4 to 1.8). Thus four addi-
467 tional modelling experiments have been designed with four different values
468 of Q_{10} (1.5, 2, 2.5, and 3), a constant copepod abundance of 200 ind.l^{-1} ,
469 $\widetilde{Q}_C=100\%$, and $T=26^\circ\text{C}$. The duration of TS2c scenario was of two weeks.

470 3.3. Starvation experiment (TS3)

471 A 52 week scenario (TS3) has been built in order to study the survival
472 ability of ML when submitted to scarce food conditions. Carbon-limited ML
473 adults ($\widetilde{Q}_C = 50\%$ and $\widetilde{Q}_N = \widetilde{Q}_P = 100\%$), at an abundance of $1 \cdot 10^{-3}$
474 ind.l^{-1} , were initially considered in the system without any food source. After
475 different starvation periods (1, 4, 6, 8 and 12 weeks), a constant abundance of
476 prey (copepods) was introduced. These prey were characterized by a carbon
477 relative quota equal to 50% ($\widetilde{Q}_C = 50\%$) and N and P relative quotas of
478 100% ($\widetilde{Q}_N = \widetilde{Q}_P = 100\%$). Three values of copepod abundance have been

479 considered (within the range of the Mediterranean Sea), namely 2.5, 5 and
 480 10 ind.l⁻¹.

481 3.4. 0D microcosm experiments (TS4)

482 After three theoretical scenarios (TS1-TS3), we aimed to investigate ML
 483 long-term population dynamics and individual responses under dynamic en-
 484 vironmental conditions (0D microcosm experiments) using three different
 485 temperature forcings. As for light forcing, a typical seasonal temperature
 486 cycle of NW Mediterranean Sea was used to force the 0D biogeochemical
 487 model :

$$T_{ref} = \max \left(13; \left| 25 \cdot \cos \left(0.45\pi \left(\frac{t/3600 - 5000}{4380} \right) \right) \right| \right), \quad (10)$$

$$Irr = \max \left(1; \max \left(50, \left| 800 \cdot \cos \left(0.45\pi \left(\frac{t/3600 - 400}{3942} \right) \right) \right| \right) \right) \sin \left(\frac{\pi t}{12 \cdot 3600} \right) \quad (11)$$

488 where t stands for the elapsed time since the beginning of the simula-
 489 tion. In this scenario and in the following, the whole planktonic food-web
 490 is now considered (see Fig.2) and behaves dynamically. The model state
 491 variables have initial values in the same ranges as those observed in the
 492 NW-Mediterranean Sea.

493 The impact of temperature on ML physiology was investigated in three
 494 test cases : (a) test case CT : the physiological rates do not vary with tem-
 495 perature ($f_{Q10} = 1$), considered as the reference scenario ; (b) test case VT :
 496 ML grazing and growth rates vary with temperature T_{ref} according to the
 497 f_{Q10} -function given by Eq.12 ; (c) test case VT-HT : the same test case as (b)
 498 but with an ambient temperature increased by 2°C (i.e. equal to $T_{ref} + 2^\circ C$).

$$f_{Q10} = Q10^{\frac{T-15}{10}}, \quad (12)$$

499 All TS4 experiments were run for 10 years.

500 3.5. Nutrient ratio experiments (TS5)

501 Scenario TS5 has been designed to investigate the impact of the NO_3 :
 502 PO_4 ratio over the Mediterranean planktonic web in the interannual time
 503 scale. Different values of PO_4 and NO_3 were considered in these experiments
 504 which correspond to three different environmental condition that could be

505 encountered in the Mediterranean ecosystems, namely : (a) the Rhône region
506 of freshwater influence (ROFI) conditions in which both nutrient concentra-
507 tions are high ($NO_3 = 5\mu M$, $PO_4 = 0.25\mu M$) and the $NO_3 : PO_4$ ratio
508 equals 20 (test case HN-LNP); (b) ROFI conditions in which NO_3 concen-
509 tration is still high ($NO_3 = 5\mu M$) but that of phosphate is lower than in the
510 previous case ($PO_4 = 0.125\mu M$), leading to a $NO_3 : PO_4$ ratio of 40 (test
511 case HN-HNP); (c) oligotrophic conditions as encountered in most of the Me-
512 diterranean Sea ($NO_3 = 1.25\mu M$, $PO_4 = 0.0625\mu M$, and $NO_3 : PO_4 = 20$,
513 test case LN-LNP)) (d) oligotrophic conditions with a strong phosphorous
514 depletion ($NO_3 = 1.25\mu M$, $PO_4 = 0.0313\mu M$, and $NO_3 : PO_4 = 40$, test
515 case LN-HNP).

516 Water buckets of 2.5 l were considered in this scenario. The chemostat
517 was characterized by an inflow of water of 0.025 l.d^{-1} with constant nutrient
518 concentrations. Nutrient inflow was temporarily stopped when the level of
519 NO_3 in the chemostat was higher than $10 \mu M$. The duration of each expe-
520 riment was 10 years.

521 3.6. Experiments on competitive pressure on ML food (TS6)

522 The invasive ctenophore ML has a strong reputation as a threat to fish
523 stocks. Negative consequences for zooplanktivorous fish due to ML predation
524 impact on the zooplankton have been observed in various ecosystems (Wag-
525 gett and Costello 1999 Shiganova & Bulgakova, 2000; Kideys & Romanova
526 2001; Purcell et al. 2001; Shiganova et al. 2001, Madesen & Riisgard, 2010,
527 Gucu et al., 2002).

528 Scenario TS6 aims to identify the competitive impact on copepods
529 by ML competitors, including a small pelagic fish, on the food-web dynamics,
530 and specifically on that of ML. This is done through the specific quadratic
531 mortality rate f_Z^{mq} (Appendix B, Table 2 in Alekseenko et al, 2014), which
532 implicitly represents in the model the level of competitive pressure exerted
533 on copepods. Three different values of f_Z^{mq} of copepods have been used, na-
534 mely $3 \cdot 10^{-8}$, $6 \cdot 10^{-8}$ and $9 \cdot 10^{-8} \text{ l.ind}^{-1} \cdot \text{s}^{-1}$, which respectively correspond to
535 the test cases referred to as LFP (same as VT case), MFP and HFP test
536 cases. Higher f_Z^{mq} values correspond to higher competitive pressure on cope-
537 pods, thus to stronger competition between other organisms and ML for the
538 available food. This could also be seen as higher fish recruitment or lower
539 fishing catchment. Here we do not take into account a case when ML itself
540 exerts a pressure on fish eggs and larvae, which could happen in nature un-
541 der some special conditions, as discussed by Cowan & Houde (1993). This

542 scenario again mimics a microcosm experiment for which temperature and
543 light forcings describe the same seasonal cycles as those given by eq. 10 and
544 11 respectively. The duration of each experiment was 36 months.

545 4. Results

546 Results obtained from the scenarios described in section 3 are presented
547 in this section in separate subsections for each scenario.

548 4.1. Effective functional response experiment (TS1 results)

549 Eleven numerical experiments were run to calculate the effective (i.e. si-
550 mulated) functional responses at steady state and compare them to the theo-
551 retical one (Fig.4). These experiments enable us to verify that the simulated
552 feeding rates produce a functional response which is similar to the theoret-
553 ical one used in the model. The model also delivers the functional response
554 expressed in terms of biomass ($\text{molC.ind}^{-1}.\text{h}^{-1}$), which is a function of the
555 prey carbon content. Red dotted lines in Fig. 4 show the envelope of possible
556 functional responses when the prey carbon relative quota varies from 0% to
557 100%. For instance, the model predicts a feeding rate of $2.7 \text{ ind.ind}^{-1}.\text{h}^{-1}$
558 when the copepod abundance equals 50 ind.l^{-1} . This corresponds to a fee-
559 ding rate expressed in carbon biomass varying from $0.7 \cdot 10^{-6}$ to $1.8 \cdot 10^{-6}$
560 $\text{molC.ind}^{-1}.\text{h}^{-1}$, depending on the nutritional status of copepods.

561 In Fig. 4b, the nutrition rate at $Z=250 \text{ ind.l}^{-1}$ with Q_C^{min} (which approxi-
562 mately reaches the saturation rate for Q_C^{min}) is equivalent to the nutrition
563 rate at $Z=25 \text{ ind.l}^{-1}$ with the Q_C^{mean} (slightly above half-saturation rate for
564 Q_C^{mean}) and at $Z=12 \text{ ind.l}^{-1}$ with Q_C^{max} (slightly below the half-saturation
565 rate for Q_C^{max}).

566 Fig.4c shows the functional response for different prey biomasses (i.e. for
567 different combinations of prey abundance times internal C quota). From this
568 figure, it is seen that ML feeding depends on the quality of the encountered
569 prey. For example, for a given prey biomass of $7.5 \cdot 10^{-5} \text{ molC.l}^{-1}$ and a
570 given ML ingestion rate (in $\text{ind.ind}^{-1}.\text{h}^{-1}$), a variety of ML feeding rates (in
571 $\text{molC.ind}^{-1}.\text{h}^{-1}$) could be calculated, ranging from $1.05 \cdot 10^{-6} \text{ molC.ind}^{-1}.\text{h}^{-1}$
572 when preys have an internal carbon quota of 0%, to $2.4 \cdot 10^{-6} \text{ molC.ind}^{-1}.\text{h}^{-1}$
573 for preys with a carbon internal content equal to 100%. Thus, the richer are
574 the prey (i.e. when their internal quota is high), the higher is the ingestion
575 rate in $\text{molC.ind}^{-1}.\text{h}^{-1}$.

576 4.2. Impact of diet on ML population growth and dynamics (TS2 results)

577 TS2a numerical experiments consider ML predation on copepod prey
 578 fixed at a given abundance level. Corresponding results are summarized in
 579 Fig. 5 and Table 4. Time evolution in ML abundance and carbon relative
 580 quota (\widetilde{Q}_C) delivered by TS2a simulations are shown in Fig. 5. Starting with
 581 an initial cohort of immature ML adults fed with different copepod prey le-
 582 vels, ML individuals reach the mature adult stage (i.e. when $\widetilde{Q}_C \geq 0\%$, cf
 583 section 2.4.2) after periods of time (t_{rep} in Table 4) varying from 12.2 hours
 584 (for the prey level of 250 ind.l⁻¹) to 129 h (for the prey level of 5 ind.l⁻¹). The
 585 abundance of the ML cohorts over the simulation initially decreases (Fig.5d)
 586 as long as the individual \widetilde{Q}_C is negative, which lasts for a longer or shorter
 587 time depending on the food level, and then increases as soon as reproduction
 588 occurs and exceeds the mortality rate.

589 The prey level of 2.5 ind.l⁻¹ does not allow any positive population
 590 growth. In this case, reproduction never occurs, since ML's \widetilde{Q}_C remains ne-
 591 gative until the end of simulation (\widetilde{Q}_C decreases down to -8.5%). This means
 592 that its internal quota Q_C is below Q_C^{min} due to higher carbon losses (asso-
 593 ciated with respiration, excretion and mortality) than carbon gains obtained
 594 through grazing.

595 The abundance of the ML population reached at the end of the simulation
 596 (i.e. when steady state is reached) increases with copepod prey abundance
 597 through an asymptotic law, reaching after 12 weeks a maximum value near
 598 1.4 ind.l⁻¹ with a carbon internal quota of 41% (Fig.6).

599 Table4 summarizes model results of TS2a through the three indicators,
 600 namely t_{rep} and SGR, previously defined (see section 2.3), and Fl_Q . The term
 601 $Fl_Q = (1 - \sigma) Q_C^{min} / t_{rep}$ corresponds to the carbon quantity accumulated in
 602 immature ML adults before reaching the mature adult stage. It is equivalent
 603 to the time-integrated balance of all simulated carbon fluxes (feeding - res-
 604 piration - excretion - mortality - quadratic mortality) of ML. Fl_Q is positive
 605 beyond a food prey level of 5 ind.l⁻¹, and increases with food abundance. The
 606 SGR, which can also be interpreted as the number of new (immature) ML
 607 individuals per adult and per hour, increases with prey level and reaches 18.3
 608 % per hour when food availability is 250 ind.l⁻¹. According to the model, in
 609 the Mediterranean where copepod abundance ranges from 2.5 to 10 ind.l⁻¹,
 610 ML SGR is up to 0.0105 per hour, i.e. 25.2 % per day.

611 Fig. 7 shows the temporal dynamics over one year of ML carbon quota
 612 and abundance for a constant carbon biomass of copepods equal to $7.5 \cdot 10^{-5}$
 613 molC.l⁻¹. From this figure, it can be seen that, for the same food biomass,

614 different dynamics of ML abundance and ML quotas can be calculated ac-
615 cording to the carbon quota of copepods. The test with the lowest copepod
616 abundance (but the richest carbon quota) leads to the highest ML abundance
617 as well as the highest carbon quota (Fig.7).

618 Conversely, the test with the highest copepod abundance (but with the
619 lowest quota) leads to the lowest ML abundances and lowest ML quotas. The
620 difference between these two extreme cases is significant : ML abundances
621 at steady state differ by around 42% and ML internal carbon quota by 25%.
622 The time necessary to reach steady state also varies according to the quality
623 of the food, from about 6 months for the carbon-poorest copepods to about
624 4 months for the carbon-richest copepods.

625 From Fig.8 it can be seen how the SGR of mature and immature ML vary
626 with temperature and food concentration (Figs.8a-b) and with Q_{10} (Fig.8c),
627 thereby allowing to estimate an envelope where SGR varies depending on
628 these conditions. Figs.8a-b show estimations of SGR depending on the tem-
629 perature conditions. It can be seen that for a given temperature, SGR of im-
630 mature ML is always 20-40% higher than SGR of mature ML. This difference
631 between SGR of mature and immature ML is decreasing with temperature
632 increase. In both cases (for mature and immature ML, Fig.8a and Fig.8b)
633 SGR is increasing with temperature. For mature ML, SGR varies from 0.1
634 d^{-1} (at 11°C) to 0.39 d^{-1} (at 26°C), for the immature ML - it is from 0.16
635 d^{-1} (at 11°C) to 0.55 d^{-1} (at 26°C). SGR increases with food increase.

636 Another temperature-related parameter impacting ML physiology is Q_{10} .
637 For the experiment TS2c with the highest temperature and food concen-
638 tration (green triangles on Figs.8a-b), we studied the impact of Q_{10} among
639 values within the range 1.5-3 : for the food concentration of 200 ind.l^{-1} with
640 $\widetilde{Q}_C=100\%$ and a temperature of 26°C . This figure shows that there is a cor-
641 relation between Q_{10} and SGR. SGR of immature ML is higher than SGR of
642 mature ML.

643 4.3. Starvation experiment (TS3 results)

644 In scenario TS3 (Fig. 8), we analyze ML individual and population res-
645 ponses to different starvation periods (from 1 to 12 weeks), followed by food
646 replenishment at three different constant abundances : 10 ind.l^{-1} , 5 ind.l^{-1}
647 and 2.5 ind.l^{-1} (the internal carbon quota of copepods is the same in all
648 experiments $\widetilde{Q}_C = 50\%$). For the three food levels, ML carbon relative quota
649 (\widetilde{Q}_C) decreases as long as starvation lasts (Fig. 8a, c and e). From food reple-
650 nishment time, \widetilde{Q}_C increases up to a stationary value, similar for a given food

651 level whatever the starvation duration, but which varies with this food level :
652 13.5% for $Z=10 \text{ ind.l}^{-1}$, 5.2% for $Z=5 \text{ ind.l}^{-1}$ and -8.5% for $Z=2.5 \text{ ind.l}^{-1}$
653 (respectively Fig. 8 a, 8c and 8e). It is worth noting that the increase in ML's
654 \widetilde{Q}_C after food reintroduction is all the more rapid in that food level is high
655 (Fig. 8a, c and e). During the first week of starvation, the initial reserves of
656 ML individuals allows the maintenance of a positive \widetilde{Q}_C , and ML population
657 abundance still increases. Beyond this period, \widetilde{Q}_C becomes negative and re-
658 production stops. Consequently, ML population abundance decreases as long
659 as starvation continues, and even after (Fig. 8b, d and f). When food is rein-
660 troduced (at time t_1) after the starvation period, the ML population does
661 not respond immediately and ML abundance still decreases as long as \widetilde{Q}_C
662 is negative. As soon as \widetilde{Q}_C becomes positive (at time t_2), ML reproduction
663 restarts, and ML population abundance increases again. Table 5 summarizes
664 the time delays ($t_2 - t_1$) between food introduction and the beginning of
665 ML population reproduction, for the two highest levels of food abundance
666 for which \widetilde{Q}_C reach positive values after food reintroduction. This time de-
667 lay non-linearly increases with the starvation duration following a saturation
668 curve and decreases with the level of food (results not shown).

669 For the starvation experiments with the highest food levels (10 and 5
670 ind.l^{-1} in Fig. 8b, and d), the time to recover the initial conditions of po-
671 pulation abundance is much longer than the starvation duration, whatever
672 this duration. Moreover, the slope of the population increase after food re-
673 plenishment is rather constant whatever the starvation history, but increases
674 with the food level. For the highest food abundance (i.e. 10 ind.l^{-1} , Fig.9b),
675 the increase in ML population reaches more or less rapidly a plateau (10
676 ind.l^{-1}), depending on the starvation duration. In the experiment with the
677 lowest food level (2.5 ind.l^{-1}), the population continues to decrease even after
678 food reintroduction (Fig.9f).

679 4.4. *OD microcosm experiments (TS4 results)*

680 Results relative to the temperature impact on the modeled food-web (see
681 Fig.2), and especially on ML and copepods, are shown in Fig.10. During the
682 simulation, the lower trophic levels (from bacteria to microzooplankton) were
683 abundant throughout the simulated period and biomass concentrations were
684 not significantly affected by the higher trophic levels (results not shown).
685 The carbon relative quota (\widetilde{Q}_C) of copepod was always close to 100%, the-
686 reby revealing the absence of C-limitation during the simulation (results not

687 shown). Hence it can be considered that during these experiments, copepod
688 and ML were in rich carbon conditions.

689 Fig.10 shows the 10-year dynamics of copepod and ML abundances and
690 of ML \widetilde{Q}_C , for the three cases presented in section 3.4 (i.e. CT, VT, and VT-
691 HT). When temperature has no impact on ML process rates (case CT), the
692 dynamics of copepods and ML are quasi-periodic, with a period that seems
693 to increase with time. For this experiment, the copepod abundance varies
694 in the range 0.5-5.5 ind.l⁻¹ (this also corresponds to the NW Mediterranean
695 copepod range). For ML, its \widetilde{Q}_C is in the range -35 – 15% and its abundance
696 varies between $5 \cdot 10^{-7}$ and 16 ind.l⁻¹.

697 During the first three years, the dynamics simulated by the two experi-
698 ments in which temperature impacts ML process rates (i.e. VT and VT-HT
699 cases) are quite similar, but they significantly differ from the CT case. These
700 dynamics do not reveal any periodicity and seem to be chaotic. After three
701 years of simulation, the patterns provided by VT and VT-HT cases begin to
702 differentiate. From year 5, the difference in terms of amplitude and frequency
703 of the abundance signals becomes very significant.

704 According to Fig.10b, when copepod abundance drops below ~ 2 ind.l⁻¹
705 (we recall that the copepod carbon content is maximum throughout the
706 simulation), ML \widetilde{Q}_C becomes negative, thereby increasing ML mortality (see
707 for example, the second half of the first year). This phenomenon is more or
708 less pronounced over the course of the 10 years of simulation (see for example
709 the very strong decrease in ML observed during the second half of the 7th
710 year for the VT case).

711 For the three cases, the lower the abundance of copepods, the lower ML
712 \widetilde{Q}_C is. It can also be seen that the higher ML mortality, the stronger ML
713 abundance decline is, and the longer the period of ML recovery is after co-
714 pepod stock replenishment. The period of ML recovery can last from 1 to
715 2 years (see for example, between years 1 and 2 for VT and VT-HT cases,
716 or between years 7 and 9 for VT case, where ML abundance is below 10-20
717 ind.l⁻¹, which can be considered as if ML was absent from the ecosystem).

718 Such successions of ML presence/absence induce shifts between food-
719 webs-with-ML to food-webs-without-ML, thereby impacting copepod dyna-
720 mics. In these cases, top down pressure dominates bottom up pressure. As an
721 example, the strong increase in ML abundance between years 6 and 7 for the
722 VT case emptied the copepod stock (Fig.10), leading, in turn, to the decline
723 in ML abundance down to $1 \cdot 10^{-37}$ ind.l⁻¹. After such a predator-prey cycle,
724 it took almost two years for copepods to recover their initial abundance value

725 and almost three years for ML.

726 In order to see whether these different abundance dynamics lead to effec-
727 tive differences in terms of ML productivity, accumulated fluxes correspon-
728 ding to the number of new individuals per liter (population growth) produced
729 during the simulated period have been calculated. The temporal variations of
730 these fluxes (i.e. accumulated abundances) as well as those of ML instanta-
731 neous abundance are presented in Fig.10e for the three experiments. During
732 the simulation, the three tests produce quite similar accumulated fluxes, cha-
733 racterized by stepping curves. The three curves remain interlaced over the
734 whole simulation, without any noticeable difference between them.

735 4.5. Nutrient ratio experiments (TS5 results)

736 Four different combinations of NO_3 and PO_4 concentrations (HN-LNP,
737 HN-HNP, LN-LNP and LN-HNP, cf section 3.5) in nutrient inflow have been
738 used in these experiments, that mimic a laboratory test in chemostat (Fig.11).
739 Note that HN-LNP and VT (see Fig.10) simulations are performed with the
740 same initial conditions and parameter values, except that VT simulation is
741 not in "chemostat mode" (no nutrient inflow occurs during the simulation).

742 Fig. 10 shows that the ML population peaks systematically following co-
743 pepod peaks in all cases except LN-HNP (see below). However, the intensities
744 of copepod and ML peaks are not correlated (see, for example, the quite si-
745 milar ML peaks in years 3 and 4 which follow copepod peaks of different
746 intensities). The delay between the maximum values of successive copepod
747 and ML peaks ranges between 40-150 days, depending on ML \widetilde{Q}_C (see star-
748 vation test TS2).

749 In the two cases of high nitrate (HN-LNP and HN-HNP where $NO_3 =$
750 $5\mu M$), relatively small differences between results are observed during the
751 first 4.5 years of simulation (Fig.11). Afterwards, these two simulations be-
752 have differently, showing shifted oscillations.

753 By contrast, for low NO_3 level ($1.25\mu M$), the experiments with low and
754 high $NO_3 : PO_4$ ratios (i.e. LN-LNP and LN-HNP) reveal strong differences
755 from the beginning of the simulation. In the condition LN-HNP, copepod
756 population first decreases and takes about 4 years to recover its initial abun-
757 dance, while ML takes about 9 years to recover. For the LN-LNP condition,
758 copepod and ML abundances deliver a quasi-periodic dynamic (around 3-
759 year period).

760 Fig.11a and b also show that ML decrease is stronger when copepod levels
761 are below 2 ind.l^{-1} . The highest ML blooms ($0.25\text{-}0.3 \text{ ind.l}^{-1}$) are observed

762 for the highest copepod levels (closer to 5.5 ind.l^{-1}), followed by a rapid
763 decline of copepod stocks. When copepod levels are close to 0 ind.l^{-1} , ML
764 rapidly decline in all the TS5 test cases. Accumulated abundances calculated
765 for the HN cases are very similar (interlaced curves). By contrast, LN cases
766 provide very different curves. For the LN-LNP case, accumulated abundance
767 is always lower than that of HN cases while it is nearly zero until year 9 in
768 the LN-HNP case.

769 4.6. Competitive predation experiments (TS6 results)

770 The impact of competitive predation in the modeled food-web is shown
771 in Fig.12. In these experiments, we investigate the impact of competitive
772 predation (implicitly represented in the model, see section 3.6) on copepods
773 and ML dynamics. The copepod abundance dynamics is highly impacted by
774 this parameter.

775 The lowest competitive predation rate case (LFP test case) induces high
776 fluctuations in the dynamics of copepods, allowing abundance values to be
777 reached as high as $5.5\text{-}6 \text{ ind.l}^{-1}$ and as low as nearly 0 ind.l^{-1} . By contrast,
778 the copepod abundance remains nearly constant (around 2 ind.l^{-1}) for the
779 highest predation rate case (HFP test case) and fluctuate between 1 and 3
780 ind.l^{-1} for the intermediate case (MFP test case).

781 Competitive predation rate also impacts ML dynamics. In all experiments
782 ML survives, but shows more fluctuating abundances (including stronger
783 blooms) when competitive predation rate is low. The more predation by
784 other organisms and fish on copepods increases, the weaker are amplitudes
785 of ML abundance fluctuations, thereby reducing outbreak occurrences.

786 5. Discussion

787 Model skill assessment

788 To be helpful for the understanding of various characteristics of ML po-
789 pulation dynamics observed in nature, under specific conditions, the model
790 had first to be assessed. These characteristics include the duration and the
791 frequency of ML outbursts, the orders of magnitude and the maximum am-
792 plitude of ML abundances, and the rate of ML population increase.

793 It was first found both for observations (from various ecosystems including
794 ML native and non-native) and in our model simulations that ML outbursts
795 do not last more than 2-3 months (Shiganova et al, 2011, Boero et al., 2013,
796 Lukas et al., 2011, Purcell et al., 2001). Moreover, as a first approximation,

797 model outputs from the 3-month long experiments with imposed constant
798 food for ML (test series TS2) can be compared to ML observations from
799 various ecosystems where ML is established.

800 In the ML native ecosystem of Narragansett Bay, over 2.5 months per
801 year, ML blooms with average abundances reaching about 10^{-2} - 10^{-1} ind.l⁻¹
802 can be observed, associated with average zooplankton concentrations in this
803 area in the range 10-100 ind.l⁻¹ (Costello et al., 2012). For such food levels,
804 the model calculates ML abundances in a consistent but wider range (10^{-3} -
805 1 ind.l⁻¹, see Fig.5c). According to the model, in ML non-native ecosystems
806 with average copepod concentrations below 3 ind.l⁻¹, characterizing oligo-
807 trophic offshore waters of the Mediterranean Sea, ML has no possibility of
808 blooming, since its physiological demands are much higher than the available
809 food (see light blue curve on the Fig.5c). This is in agreement with several in
810 situ studies (Ghabooli et al., 2013, CIESM, 2014, Fuentes et al., 2010), sho-
811 wing that ML was not found in such areas. If we consider the Mediterranean
812 coastal areas, which are much richer in zooplankton, with concentrations hi-
813 gher than 10 ind.l⁻¹, the simulated ML abundance is in the order of 10^{-3}
814 ind.l⁻¹ (see magenta curve in Fig.5c and lines for higher food concentration).
815 This order of magnitude of ML abundance can also be found, for example,
816 in the Black Sea in recent years (Shiganova et al., 2018) and in the Sea
817 of Marmara (Isinibilir et al., 2004). For the highest food concentration of
818 25-250 ind.l⁻¹, simulated ML abundance is in the range $5 \cdot 10^{-2}$ - 1 ind.l⁻¹
819 (Fig.5c); this is in agreement with ML abundances measured in the Black
820 Sea, Azov Sea and Caspian Sea (Shiganova, personal communication). In
821 conclusion, our model could reproduce the orders of magnitude of ML abun-
822 dances observed in various ecosystems differing by their eutrophisation and
823 zooplankton levels.

824 Modeled SGR values can also be compared to the measured ones in dif-
825 ferent studies (Reeve et al., 1989, Purcell et al., 2001, Finenko et al., 2000,
826 2006, Larson, 1985). The values of SGR found by these authors are quite
827 different, mainly due to the specific experimental conditions, such as (i) im-
828 posed copepod levels (in Reeve et al., 1989 and Purcell et al., 2001, the levels
829 are the same : 20, 50, 100 and 200 ind.l⁻¹; in Finenko et al., 1995, the levels
830 are in the range 60-100 ind.l⁻¹.), (ii) temperature conditions (in Reeve et al.,
831 1989 and Purcell et al., 2001, it is 26°C; in Finenko et al., 2006 11°C and
832 14°C.), (iii) ML age/size chosen for the experiment (in Reeve et al., 1989,
833 it corresponds to mature ML, in Purcell et al., 2001 - to immature ML; in
834 Finenko et al., 2006 - to mature and immature ML), (iv) ML taken from

835 different locations (from Narragansett Bay in Reeve et al., 1989 and Purcell
836 et al., 2001, from the Black Sea in Finenko et al, 2000, and from the Caspian
837 Sea in Finenko et al, 2006), and also (v) water container sizes chosen for ex-
838 periment and conversion parameters (from carbon biomass, wet weight, dry
839 weight, etc).

840 The values of SGR estimated in these experiments are within the range of
841 $0.43-0.87 \text{ d}^{-1}$ - for immature ML at the highest temperature (at 26°C) (Pur-
842 cell et al., 2001, corresponding to copepod abundance range $20-200 \text{ ind.l}^{-1}$)
843 and in the range of $0.23-0.34 \text{ d}^{-1}$ for the same food quantities for mature
844 ML (Reeve et al., 1989, Purcell et al., 2001); for the lower temperatures
845 ($11-14^{\circ}\text{C}$), values of SGR are around 0.07 d^{-1} (Finenko et al., 2006, in the
846 Caspian Sea). Larson (1985) estimated SGR of ML in natural waters (in
847 different waters of U.S.) in the range $0.1-0.3 \text{ d}^{-1}$ (see his Table 4).

848 TS2c numerical experiments were designed to take into account all these
849 conditions, not only for model skill assessment through comparison with data,
850 but for a better understanding of the impact of each of these factors on ML
851 SGR. Food and temperature are known to have the greatest impact on ML
852 dynamics (Costello et al., 2012). Temperature impacts ML exponentially
853 (through the Q_{10} -function), where the Q_{10} -function is a function of tempe-
854 rature and Q_{10} parameter, which is estimated in situ.

855 Modeled SGR shown in Figs.8a-b with $Q_{10}=1.5$ gave an SGR range of
856 $0.1-0.39 \text{ d}^{-1}$ for mature ML and of $0.16-0.55 \text{ d}^{-1}$ - for immature SGR, both
857 increasing with temperature and food concentration. These values are within
858 the same order of magnitude as the measured SGR, but slightly underesti-
859 mated for the highest temperature when compared to the measured tempe-
860 ratures given in Reeve et al. (1989) and Purcell et al. (2001). In order to
861 go further, we performed additional numerical experiments for the highest
862 food concentration and temperature with varying Q_{10} values (Fig.8c). Fig.8c
863 shows that the modelled SGR is highly dependent on Q_{10} . SGR is increased
864 from 0.39 d^{-1} to 0.92 d^{-1} for mature ML, and from 0.55 d^{-1} to 1.1 d^{-1} for
865 immature ML when Q_{10} varies from 1.5 to 3. The range of modeled SGR
866 with varying Q_{10} is wider, and it now includes the values found by Reeve et
867 al. (1989) and Purcell et al. (2001).

868 Few long term observations of ML exist (Purcell et al. 2001), mainly
869 along the East coast of North America, in the Narragansett Bay (Beaulieu
870 et al., 2013) and in the Chesapeake Bay (Miller, 1974; Purcell et al. 2001),
871 and in the Black sea (Shiganova, 2001; Kideys et al., 2000, Finenko et al.,
872 2013). If well settled ML populations in deep bays appear every year, obser-

873 vations in coastal or oceanic areas show irregular peaks of abundances both
874 in frequency and intensity. CIESM (2015) mentions that the winter biology
875 of ML is a key parameter to understand population dynamics, as it does not
876 present benthic resting stages (Rapoza et al., 2005; Boero et al. 2008). Its
877 survivability is due to its good resistance to long term starvation combined
878 with an ability to restore growth and reproduction as soon as conditions are
879 favorable. As ML is able to self-fertilize (Baker & Reeve 1974; Sasson &
880 Ryan, 2016), extremely low densities of individuals may not affect reproduc-
881 tion capabilities, whereas small-sized individuals are able to mobilize matter
882 for reproduction (Finenko et al., 2006; Jaspers et al., 2011). Therefore, a
883 population reserve with extremely low-density of small individuals might be
884 the seed of later new population outbreaks; probably in successive phases
885 of population growth, when water temperature and resource abundances al-
886 low out-crossing reproduction and large-sized spawning individuals (Costelo
887 et al. 2006; Sasson and Ryan, 2016). Several features of our long term si-
888 mulations (see our Fig. 10) reproduce observed biological patterns of ML
889 dynamics. One property of our model is its capacity to reproduce such popu-
890 lation dynamics variations (outbreaks and disappearance) without changing
891 the parametrization of physiological and demographic processes. Although
892 our seasonal pattern of temperature was a regular forcing function, the inter-
893 actions between plankton dynamics and ML population induced chaotic-like
894 dynamics of outbreaks. Moreover, our model seems able to reproduce the
895 general properties characterizing ML peaks of abundances as observed in va-
896 rious ecosystems, such as the 2-3 months duration of such peaks, the order
897 of magnitude of ML abundances found in native and non-native ML ecosys-
898 tems. Our simulations suggest that the match or mismatch with the prey,
899 and the high SGR and reproduction rates, increased at high temperatures,
900 are the main factors inducing ML outbreaks. Conversely, long phases of near-
901 absence of simulated ML individuals are due to a collapse of ML population
902 followed by several years needed to recover a sufficient stock to make possible
903 new outbreaks when matching with a planktonic prey production phase.

904 Finally, other factors liable to strongly modify ML outbreaks that are
905 not taken into account in our study are coastal hydrographic retention of
906 individuals, mainly during winter time (Kremer & Nixon, 1976; Beaulieu et
907 al., 2013; Costello et al, 2012), and the presence of ML predators such as
908 *Beroe ovata* (Shiganova et al., 2001).

909 **Functional response and reproduction function**

910 The functional response is an essential specific life trait conditioning many

911 aspects of the species survival and prosperity ML functional response is the
912 first factor that has been investigated in this paper aiming at improving our
913 understanding of the conditions favoring ML development and outbreaks.
914 First, it must be noted that there is a general confusion in the definition and
915 use of the concept of functional response (which can be expressed either in
916 abundance or in biomass). The initial concept (ref : Holling cf paper Capparoy
917 & Carlotti, 1996) deals with numbers of ingested prey vs individual prey
918 concentrations, but biogeochemical models usually use a mass currency, i.e.
919 ingested mass of prey vs prey biomass concentrations (Carlotti & Poggiale,
920 2010). An interesting property of the model used in this study is that it
921 allows to delivery of the functional response in all possible combinations of
922 units with prey density expressed either in individual abundance or biomass
923 concentration per liter, and feeding rate in abundance or biomass of consumed
924 prey per predator per unit time (see Fig 4).

925 Generally, the variations in the functional response types are attributed
926 to (i) the prey species composition, (ii) the range of size (or stage) of prey
927 and predators and the associated swimming behavior, (iii) the patchiness
928 and/or the relative densities of prey and predators and any environmental
929 parameter affecting patchiness, since these factors are considered to modify
930 the different parameters of the functional responses (i.e. attack rate, handling
931 time, satiation, see for instance Capparoy & Carlotti, 1996 for details). In
932 addition to all these factors, this study highlights the importance of the nu-
933 tritional status of prey when handling functional responses where relatively
934 lower concentrations of prey can be compensated by high nutritional values,
935 as shown in Fig. 4.

936 Fig. 4 also shows that to a given functional response expressed in abun-
937 dance (available prey and consumed prey) corresponds an infinity of func-
938 tional responses in biomass located in an envelope that is generated by all
939 the possible nutritional states of prey. The same conclusion could be drawn
940 for a given functional response expressed in biomass, which can correspond
941 to a variety of functional responses expressed in terms of prey abundances,
942 according to the nutritional quality of the prey (up to a tenfold increase or
943 decrease in the present example).

944 Furthermore, the shape of the functional response expressed in biomass
945 (here type 2, Fig. 4b) is identical to that of the functional response expressed
946 in abundances (Fig. 4a) because a constant quota of carbon has been conside-
947 red for each simulation. When the prey quota varies in addition to abundance
948 (which is a realistic situation), the shape of the functional response expressed

949 in biomass can be of any other type because the values of ingestion rate may
950 fall anywhere between the two envelopes. All this suggests that a full charac-
951 terization of the functional response requires the experimental determination
952 of two functional responses : one expressed in terms of individual abundances
953 and the other in terms of biomass.

954 In the NW Mediterranean, the average copepod abundance range is ge-
955 nerally below 10 ind.l^{-1} , more often in the range $1\text{-}2 \text{ ind.l}^{-1}$ in the open sea
956 (e.g. Nowaczyk et al., 2011 ; Donoso et al., 2017 both using $120 \mu\text{m}$ mesh size
957 nets), with generally higher values on shelves and coastal zones (Espinasse
958 et al., 2014, 2017). In this range of prey abundance, ML functional response
959 is almost linear (type I), varying from 0 to $1 \text{ ind.ind}^{-1}.\text{h}^{-1}$ and from 0 to
960 $0.6 \text{ molC.ind}^{-1}.\text{h}^{-1}$ (Fig.4b). This suggests that ML generally starves in the
961 NW Mediterranean Sea due to low food concentrations in oceanic waters.
962 However, ML ingestion rate increases rapidly in the food range $10\text{-}50 \text{ ind.l}^{-1}$.
963 This could explain ML's establishment in more productive Mediterranean
964 littoral regions and coastal lagoons (Fuentes et al. 2010 ; Delpy et al, 2016,
965 Shiganova et al, 2014, Pitois & Shiganova, CIESM, 2015). In the first part of
966 the curve (Fig.4), the functional response slope is steep, and therefore preda-
967 tion on copepods is very strong relative to their abundance : the percentage
968 of ingested copepods per hour correspond to 10% of the population when
969 the abundance of copepods is low, while this percentage drops to 1.7% when
970 the abundance of copepods is high. This may explain sudden switchovers
971 (stiff dynamics) between populations of copepods and ML obtained at low
972 copepod concentrations obtained in experiments TS3-TS5 (Figs. 9-11).

973 **Impact of the prey quality on ML ingestion rate and ML dyna-** 974 **mics**

975 Fig.4c shows that for a given prey biomass (i.e. for different combinations
976 of prey abundance times prey internal C quota), the richer the prey (i.e. the
977 higher the internal quota), the higher the ingestion rate (in $\text{molC.ind}^{-1}.\text{h}^{-1}$)
978 is. This suggests that ML feeding highly depends on the quality of the encoun-
979 tered prey. As a consequence, ML dynamics also depends on the nutritional
980 quality of prey. An important result is that for a given fixed available prey
981 biomass, ML abundance is maximum for the prey of richest nutritional values
982 (see Fig.7). In the TS2 scenario, we tested the ability of immature ML adults
983 to reach the sexual maturity for different fixed food levels. We have found
984 that for high level of copepods (5 ind.l^{-1} and more), ML juveniles take less
985 than 1 week to reach their sexual maturity. The food level of 2.5 ind.l^{-1} is
986 critical, since in this case and for lower food concentrations, ML never reach

987 sexual maturity. This is due to the predominance of biomass losses compared
988 to gains by predation. Therefore, according to these model results, it could be
989 supposed that, in ecosystems with low food conditions (i.e. below 5 ind.l⁻¹),
990 ML reproduction is very unlikely to occur. This result is also consistent with
991 experimental data showing that at natural prey densities below 4 copepods
992 per liter, ML is not satiated (Reeve et al., 1989).

993 The model considers two levels of ecological integration : individual and
994 population. For a given food level (in TS2 only prey abundance varies but
995 not their internal quota), surviving ML individuals reach the same internal
996 quota whatever the starvation duration (Fig.9a, c, e), and this quota value
997 depends on the food level. In the same way, for a given food level, the ML
998 population will reach the same abundance whatever the starvation duration
999 (reached beyond the time period presented in Fig.9). However, it can be seen
1000 that the response to starvation occurs at different time scales depending on
1001 the integration level : the stationary quota of ML individuals is reached by
1002 survivors after a few weeks, while it takes several months or even years for the
1003 ML population to “forget” the starvation period and recover its initial abun-
1004 dance value. Finally, the period necessary to reach steady state conditions
1005 will increase with the starvation duration.

1006 Moreover, for short starvation periods (one week), ML individual and
1007 population growths were barely affected by starvation in the case where food
1008 recovery is sufficient (i.e. Z equal or higher than 5 ind.l⁻¹, see Fig.9a, c, e).
1009 The same phenomenon for short starvation periods have been observed in the
1010 laboratory-controlled experiments performed by Jaspers et al. (2015). These
1011 authors found that starved ML continue to reproduce for up to 12 days after
1012 cessation of feeding, with high overall hatching success of 65–90%.

1013 For longer periods of starvation, ML population abundance will be af-
1014 fected. This impact is however likely overestimated by the model since, in
1015 natural conditions, population response to long term starvation induces new
1016 forms of resistance (latency stage, dormancy, etc) which will potentially limit
1017 the population mortality.

1018 **Characteristics of ML dynamics impacting population blooms**

1019 TS3 scenarios at the scale of one year illustrate that, even under stable
1020 environmental (i.e. light and temperature) conditions, depending on the star-
1021 vation duration, the ML population will bloom or not in the current year (see
1022 Fig.9). This is a supplementary source of irregularity in ML dynamics and
1023 in the occurrence of ML outbreaks.

1024 In the case of varying environmental conditions through the introduction

1025 of light and temperature seasonal variations (TS4), model results showed
1026 that, the more the ML population drop is important, the longer the delay
1027 is before it restores (see Fig.10 and the following). The nature of this re-
1028 lationship between the minimum value reached by the abundance and the
1029 restoring time is worth understanding. As seen in Fig. 9e, near zero values
1030 of ML abundance can be interpreted as a total disappearance of ML with
1031 the linear scale. Only a logarithmic representation (Fig. 9d) offers a means
1032 to highlight differences between those different near zero ML abundances.
1033 These low concentrations of ML (below 0.1 ind.m^3) are spread over several
1034 orders of magnitude (from 10^{-1} to 10^{-35} ind.m^3). Although these very low
1035 abundances are all considered as an absence of ML for any observer, it turns
1036 out that they have a major impact on the timing of the reappearance of ML
1037 when food conditions become again favorable. In our tests TS4, TS5 and
1038 TS6, the duration between two ML outbreaks can typically vary between 1
1039 and 3 years (Fig.10d).

1040 **Forcings impacting ML population growth**

1041 In this work, three major conditions impacting ML dynamics through the
1042 predation pressure on copepods were studied : light irradiance, water tempe-
1043 rature, nutrient availability . In the model, only water temperature directly
1044 impacts ML physiology, when all forcing conditions impact ML resources
1045 (lower trophic levels and/or copepod).

1046 Regarding the effect of water temperature, the conclusions are not straight-
1047 forward (Fig.10) and depend on the criteria selected for analysis. If the cri-
1048 terion is the number of ML bloom occurrences, it is higher in the VT-HT
1049 case (9 outbreaks in 10 years) than in the CT (8 outbreak events) and VT
1050 (6 outbreaks) cases. This means that an increase in the mean temperature
1051 may promote the occurrence of jellyfish outbreaks. Now, if we consider the
1052 integrated amounts of jellyfish produced over 10 years (Fig.10), the impact
1053 of temperature seems less clear since occurrences of jellyfish in the VT and
1054 CT simulations are rare but are compensated by higher amplitudes of the
1055 different peaks.

1056 The impact of $NO_3 : PO_4$ ratio is noticeable at low NO_3 concentration
1057 since in the corresponding simulations, ML abundance decreases from the
1058 beginning of the simulation and for several years (Fig.11b). This long per-
1059 iod with lower predation on copepods enables them to grow and reach an
1060 abundance level sufficient for the re-occurrence of an ML bloom. Depending
1061 on the levels of NO_3 and PO_4 concentrations, different numbers of blooms
1062 occurred : six outbreaks for HN-HNP case, six for the HN-LNP case, three

1063 for the LN-LNP case and only one for the LN-HNP case. For the highest
1064 NO_3 concentration, the same number of outbreaks is simulated whatever the
1065 $NO_3 : PO_4$ ratio, while for the lowest NO_3 concentration, there are more
1066 outbreaks for the low $NO_3 : PO_4$ ratio (three outbreaks for LNP against
1067 only one for HNP). This could be explained by the fact that in the former
1068 case, copepods dynamics are quite similar for HNP and LNP cases (Fig.11a),
1069 while in the latter case major changes in the low trophic levels (not shown)
1070 significantly impact the dynamics of copepods and thereby that of ML.

1071 Competitive implicit grazing pressure exerted on copepods by other orga-
1072 nisms than ML, including small pelagic fishes, plays an important role in ML
1073 population dynamics : the lowest competitive predation pressure leads to the
1074 highest integrated ML population growth over the ten simulated years, and
1075 to the alternates of periods with ML disappearance followed by strong blooms
1076 over the simulated period. By contrast, for the highest competitive predation,
1077 ML abundance remains quite low and constant though with a slight tendency
1078 to increase during the ten-year simulation. In short, according to our model,
1079 the lowest grazing pressure on copepods (which could correspond to a situa-
1080 tion of intensive fishing) produce the highest occurrence and intensity of ML
1081 blooms. By contrast, the highest grazing pressure (which could be found for
1082 low fishing activity), ML is always present but at very low concentrations.

1083 Unlike for previous experiments (TS4 and TS5), ML accumulated abun-
1084 dances are clearly different in the three simulations of experiment TS6. This
1085 is due to the fact that the total pressure (ML + other organisms) exerted
1086 on copepods is approximately constant, and that an increase in one of these
1087 two pressures necessarily reduces the other pressure. Copepod grazing by
1088 ML is indeed higher when the pressure exerted by other organisms is lo-
1089 wer, resulting in higher ML abundances. According to our simulations, the
1090 forcing with the greatest influence on ML dynamics is that of competitive
1091 grazing pressure on copepods (which could be a proxy of fishing pressure),
1092 since it significantly impacts not only the frequency of ML outbreaks, but
1093 the accumulated population growth of ML over 10 years.

1094 Similar conclusions have been drawn by Gucu et al. (2002) using different
1095 sources of observations from the Black Sea. They conclude that overfishing
1096 plays a crucial role in the successful development of ML, by emptying the
1097 ecological niche occupied by small pelagic fishes, and allowing gelatinous com-
1098 petitors to re-inhabit. The zooplankton fish pathway was blocked by heavy
1099 fishing pressure in the 1980s in the Black Sea, so the flow of excess biological
1100 material was diverted, to a large extent, in favor of gelatinous organisms,

1101 including ML. As a consequence, the fish compartments were remarkably
1102 reduced. Based on field data and the relevant literature in the Black Sea,
1103 Shiganova & Bulgakova (2000) also discussed the dramatic effect of ML on
1104 fish eggs and larvae, in terms of feeding and stocks. These authors indeed
1105 found noticeable changes in fish diet composition in absence of copepods.
1106 Moreover, when copepods were not found at all in fish stomachs, fish average
1107 length, weight, and fat content were lower, and mortality increased during
1108 winter.

1109 **Observation period : short vs long-term observation periods**

1110 In Fig. 10, during the first 3-4 years, the effects of the ratio of nutrients
1111 are barely perceptible in the cases high NO_3 cases (HN). These effects be-
1112 come significant after 4 years, not in terms of integrated quantities over the
1113 long term, but in terms of short-term amounts and number of bloom events.
1114 Shorter simulations could lead us to the conclusion that the $NO_3 : PO_4$ ratio
1115 has no impact on the food web structure at high NO_3 , while here it highlights
1116 the fact that the impact of this ratio is significant at medium- and long-term
1117 only (for example, there is a peak in ML abundance for the low $NO_3 : PO_4$
1118 ratio (LNP) in the 7th year, while there is none for the high $NO_3 : PO_4$
1119 ratio (HNP). This example (and others in this study) shows that long-term
1120 simulations are required to study and understand ML population dynamics
1121 and successions. This study suggests that the same long-term acquisition
1122 is required for in situ observations, and that the frequency of observations
1123 should not exceed one month since bloom durations do not last more than
1124 2-3 months, as suggested both by in situ observations and our model simu-
1125 lations (Shiganova et al, 2011, Boero et al., 2013, Lukas et al., 2011, Purcell
1126 et al., 2001). Moreover, it is not only the frequency of occurrence of jelly-
1127 fish which needs to be observed, but also the amplitude of these occurrences
1128 since, according to this study, the amplitude seems to partly condition the
1129 time of the occurrence of the next bloom.

1130 **Model properties and results compared to previous modelling** 1131 **studies**

1132 The model presented in this study differs from previous Mnemiopsis
1133 models in many aspects : (i) Mnemiopsis population is simply represented
1134 through a single variable; (ii) it is an enhanced flexible-stoichiometry mo-
1135 del, since organisms are also represented through individual abundances in
1136 addition to their representation through C, N and P concentrations. As a
1137 consequence, internal quotas can be calculated, thereby providing a proxy
1138 of mean individual weight for ML and other populations; (iii) a two-way

1139 coupling has been developed with the lower trophic levels from bacteria to
1140 mesozooplankton (copepods).

1141 Though our model does not include a detailed stage-structured represen-
1142 tation of ML as in Salihoglu et al., (2011) or Shiganova et al. (2018) for
1143 example, it has proved to provide a realistic description of the main indi-
1144 vidual and population properties (SGR, abundances, SPGR, etc.) and to
1145 reconstitute to a certain extent the development of cohort and the rapid popula-
1146 tion outbreaks or long-duration disappearance. Moreover, our model allows
1147 representation of the dynamics of *Mnemiopsis* population from seasonal to
1148 decadal scales in a variable trophic environment. Most of the parameters
1149 for ingestion and metabolic processes are taken from Salihoglu et al. (2011),
1150 which itself extensively used information from historical references on *Mne-*
1151 *miopsis* data and modeling (Kremer, 1976, Kremer & Reeve, 1989). However,
1152 the new feature of our model is that it represents the predator-prey functio-
1153 nal responses on the basis of densities and not biomass. Thanks to this model
1154 capacity, it has been shown, as far as we know for the first time, that for a gi-
1155 ven prey biomass, ML population growth will be higher with a lower number
1156 of C-rich prey than for a higher number of C-poor prey.

1157 Some previous modelling studies have been undertaken in a 3D confi-
1158 guration, combining a lagrangian transport of *Mnemiopsis* at regional scale
1159 with food and temperature conditions, forcing a detailed DEB model (van
1160 der Molen et al., 2015; David et al., 2015). These simulations at regional
1161 and seasonal scales are interesting, as they highlight the capability of ML to
1162 maintain low population through winter due to low temperature tolerance
1163 and starvation. However, such detailed structured population models are not
1164 suitable (accounting for computational costs) to explore the long-term dyna-
1165 mics along with the interactions with lower trophic levels through a two-way
1166 coupling with LTL. Even if the results are not shown in the present paper,
1167 the present model has already been run in a 3D regional context in versions
1168 including (Alekseenko et al., pers. comm.) or not (Alekseenko et al., 2014;
1169 Guyennon et al., 2015) the ML compartment.

1170 **6. Conclusions**

1171 In the present work, *Mnemiopsis leidyi* (ML) have been added in the
1172 trophic web described by the biogeochemical model Eco3M-MED. With this
1173 model, we investigated, through different numerical experiments and scena-
1174 rios, the impact of starvation, food availability and quality, temperature,

1175 nutrient availability and ratios and competitive pressure on ML physiology
1176 and population growth. After a thorough study of the model properties at the
1177 individual and population levels, different scenarios of climate change have
1178 been simulated in order to analyze inter-annual variability of this species and
1179 the role of environmental parameters impacting these variations.

1180 Though academic, the simulated scenarios are indeed helpful in unders-
1181 tanding the role of ML physiology and external factors on ML dynamics, and
1182 in drawing some hypotheses concerning the environmental windows leading
1183 to ML establishment and outbreaks in the natural environments, especially
1184 along the coasts of the Mediterranean Sea.

1185 Our results firstly show that the required food conditions for ML out-
1186 bursts, which involves a combination of food quality and quantity, should
1187 mainly be found in the most productive Mediterranean coastal areas and
1188 more rarely in the open sea, and that variations in food concentration may
1189 induce rapid outburst or collapse of ML populations. Results also indicate
1190 that food concentration directly impact reproduction, and that for a given
1191 fixed available prey biomass, ML abundance is maximum for the prey with
1192 the richest nutritional value.

1193 As our model considers two levels of ecological integration, individual
1194 and population, it has been shown that the response to starvation or to
1195 recovery from starvation after food replenishment occurs at different time
1196 scales, depending on the integration level : individuals react immediately
1197 to food replenishment, whereas the population's response depends on the
1198 demographic structure, mainly the presence of mature adults.

1199 Different global change scenarios have been run in order to analyze inter-
1200 annual variability in ML population dynamics (i.e. mainly the intensity and
1201 frequency of ML outbreaks), and to identify how key environmental parame-
1202 ters impact this variability. When varying some environmental factors (tem-
1203 perature, food availability and quality issued from different nutrient ratios,
1204 and competitive pressure on ML's food), ML population dynamics turns out
1205 to be rather chaotic, with the strongest ML blooms followed by the deepest
1206 population drops. The intensity of the ML population drops during starva-
1207 tion periods determines the time lapse before the reappearance of ML when
1208 food conditions become favorable again. This could explain the absence of ML
1209 during several years in the natural environment. These simulations also high-
1210 light that (i) an increase in the mean temperature promotes the occurrence of
1211 jellyfish outbreaks, (ii) through its effect on prey quality, the nutrient ratio at
1212 the basis of the primary production modifies the outbreaks frequency, mainly

1213 at low nitrate concentrations, and (iii) changes in top-down pressure on ML
1214 prey (implicitly representing changes in fishing pressure) impact not only the
1215 frequency of the outbreaks, but also the accumulated population growth of
1216 ML over a ten-year period, and seems to be the forcing most influencing ML
1217 dynamics.

1218 Since the conclusions of this work (mainly those relative to ML deve-
1219 lopment in rich coastal areas, to the low frequency and non-periodicity of
1220 presence-absence cycles,etc.) were derived from an academic study using a
1221 0D model, it would be worth checking whether these results would be confir-
1222 med in a three-dimensional model accounting for the presence of physical
1223 forcings generating spacial patchy prey and predator distributions as well
1224 as temporal variations at different scales (day, season, inter-annual, multi-
1225 decade,etc.).

1226 In addition to these results, this work gives rise to two recommenda-
1227 tions : (i) since, according to the nutritional states of prey, a given functional
1228 response expressed in abundance corresponds to an infinity of functional res-
1229 ponses in biomass, and conversely, a full characterization of the functional
1230 response for modelers would require the experimental determination of the
1231 functional response in two units : individual abundances and biomass, (ii)
1232 due to the low frequency of the ML presence-absence fluctuations, our simu-
1233 lations call for long-term (over at least a ten-year periods) observations with
1234 a temporal resolution of one month or less.

1235 **Acknowledgements**

1236 This work is a contribution to the Labex OT-Med (N° ANR-11-LABX-
1237 0061) funded by the French Government «Investissements d’Avenir» program
1238 of the French National Research Agency (ANR) through the A*MIDEX pro-
1239 ject (N° ANR-11-IDEX-0001-02). The authors acknowledge the staff of the
1240 "Cluster de calcul intensif HPC" Platform of the OSU Institut Pythéas (Aix-
1241 Marseille Université, INSU-CNRS) for providing the computing facilities.
1242 The authors gratefully acknowledge M. Libes and C. Yohia from the Service
1243 Informatique de Pythéas (SIP) for technical assistance.

1244 **References**

- 1245 [1] Alekseenko E., Raybaud V., Espinasse B., Carlotti F., Queguiner
1246 B., Thouvenin B., Garreau P., Baklouti M., 2014. Seasonal dyna-

- 1247 mics and stoichiometry of the planktonic community in the NW
1248 Mediterranean Sea : a 3D modeling approach. *Ocean Dynamics*.
1249 <http://dx.doi.org/10.1007/s10236-013-0669-2>.
- 1250 [2] Anninsky B.E., Romanova Z.A., Abolmasova G.I., Gucu A.C., Kideys
1251 A.E., 1998. Ecological and physiological state of the ctenophore *Mnemiopsis leidyi* (Agassiz) in the Black Sea in autumn 1996. In : Ivanov
1252 LI, Ozoy E (eds) NATO TU-Black Sea Project, ecosystem modeling as
1253 a management tool for the Black Sea, symposium on scientific results,
1254 Vol 1. Kluwer Academic Publishers, Dordrecht, p 249-262.
- 1256 [3] Auger P.A., Diaz F., Ulses C., Estornel C., Neveux J., Joux F., Pujo-Pay
1257 M., Naudin J.J., 2011. Functioning of the planktonic ecosystem on the
1258 Gulf of Lions shelf (NW Mediterranean) during spring and its impact
1259 on the carbon deposition : a field data and 3-D modeling combined
1260 approach. *Biogeosciences* 8 :3231–3261.
- 1261 [4] Baker L.D., Reeve M.R., 1974. Laboratory culture of the lobate cteno-
1262 phore *Mnemiopsis mccradyi* with notes on feeding and fecundity. *Mar*
1263 *Biol* 26 :57-62.
- 1264 [5] Baklouti M., Diaz F., Pinazo C., Faure V., Quequiner B., 2006a. Invest-
1265 igation of mechanistic formulations depicting phytoplankton dynamics
1266 for models of marine pelagic ecosystems and description of a new model.
1267 *Prog Oceanogr* 71 :1–33.
- 1268 [6] Baklouti M., Faure V., Pawlowski L., Sciandra A., 2006b. Investiga-
1269 tion and sensitivity analysis of a mechanistic phytoplankton model im-
1270 plemented in a new modular tool (Eco3M) dedicated to biogeochemical
1271 modelling. *Prog Oceanogr* 71 :34–58.
- 1272 [7] Baklouti M., Chevalier C., Bouvy M., Corbin D., Pagano M., Troussellier
1273 M., Arfi R., 2011. A study of plankton dynamics under osmotic stress in
1274 the Senegal River Estuary, West Africa, using a 3D mechanistic model.
1275 *Ecol Model* 222(15) :2704–2721.
- 1276 [8] Beaulieu W.T., Costello J.H., Klein-Macphee G., and Sullivan B.K.,
1277 2013. Seasonality of the ctenophore *Mnemiopsis leidyi* in Narra-
1278 gansett Bay, Rhode Island. *J. Plankton Res.* 35, 785–791. doi :
1279 10.1093/plankt/fbt041.

- 1280 [9] Boero F., Bouillon J., Gravili C., Miglietta M. P., Parsons T., Piraino
1281 S., 2008. Gelatinous plankton : irregularities rule the world (sometimes).
1282 Mar. Ecol. Prog. Ser. 356, 299–310.
- 1283 [10] Boero F., Putti M., Trainito E., Prontera E., Piraino S. & Shiganova
1284 T., 2009. Recent changes in Western Mediterranean Sea biodiversity :
1285 the establishment of *Mnemiopsis leidyi* (Ctenophora) and the arrival of
1286 *Phyllorhiza punctata* (Cnidaria). Aquatic Invasions 4 : 675–680.
- 1287 [11] Boero F., 2013. Review of jellyfish blooms in the Mediterranean and
1288 Black Sea. Studies and Reviews No.92 , General fisheries commission
1289 for the Mediterranean, ISBN 978-92-5-107457-2.
- 1290 [12] Byers J. E., 2002. Impacts of non-indigenous species on natives enhanced
1291 by anthropogenic alteration of selection regimes. *Oikos*, 97, 449–458.
- 1292 [13] Capparoy P. & Carlotti F., 1996. A model of *Acartia tonsa* : effect of turbulence
1293 and consequences for the related physiological processes. *Journal of Plankton Research* 18,
1294 2139-2177.
- 1295 [14] Carlotti F. & Poggiale J., 2010. Towards methodological approaches to
1296 implement the zooplankton component in 'end to end' food web models.
1297 *Progress in Oceanography*, 84 (1-2), 20-38, ISSN 0079-6611.
- 1298 [15] Colin S.P., Costello J.H., Hansson L.J., Titelman J., Dabiri J.O.,
1299 2010. Stealth predation and the predatory success of the invasive
1300 ctenophore *Mnemiopsis leidyi*. *Proceedings of the National Academy of Sciences of the United States of America* 107 : 17223–17227,
1301 <http://dx.doi.org/10.1073/pnas.1003170107>.
- 1303 [16] Collingridge K., van der Molen J. and Pitois S., 2014. Modelling risk
1304 areas in the North Sea for blooms of the invasive comb jelly *Mnemiopsis leidyi*.
1305 *Agassiz*, 1865. *Aquatic Invasions* 9, 21–36.
- 1306 [17] Costello J.H., Bayha K.M., Mianzan H.W., Shiganova T.A., Purcell J.E.,
1307 2012. Transitions of *Mnemiopsis leidyi* (Ctenophora : Lobata) from a
1308 native to an exotic species : a review. *Hydrobiologia* 690(1) : 21–46,
1309 <http://dx.doi.org/10.1007/s10750-012-1037-9>.

- 1310 [18] Costello, J.H., B.K. Sullivan, D.J. Gifford, D. van Keuren, and L.J. Sulli-
1311 van., 2006. Seasonal refugia, shoreward thermal amplification, and meta-
1312 population dynamics of the ctenophore, *Mnemiopsis leidyi* in Narragan-
1313 sett Bay, Rhode Island. *Limnology and Oceanography* 51 :1819–1831.
- 1314 [19] Cowan J. H. & Houde E.D., 1992. Size-dependent predation on marine
1315 fish larvae by ctenophores, scyphomedusa, and planktivorous fish. *Fish.*
1316 *Oceanogr.* 1 : 113–126, doi :10.1111/j.1365-2419.1992.tb00030.x.
- 1317 [20] Cowan J. H. & Houde E.D., 1993. Relative predation potentials
1318 of scyphomedusae, ctenophores and planktivorous fish on ichthyo-
1319 plankton in Chesapeake Bay. *Mar. Ecol. Prog. Ser.* 95 :55–65,
1320 doi :10.3354/meps095055.
- 1321 [21] David M., Gollasch S., Pavliha M., 2013. Global ballast water manage-
1322 ment and the “same location” concept : a clear term or a clear issue ?
1323 *Ecological Applications* 23 : 331–338, [http ://dx.doi.org/10.1890/12-](http://dx.doi.org/10.1890/12-0992.1)
1324 [0992.1](http://dx.doi.org/10.1890/12-0992.1).
- 1325 [22] David, C., Vaz, S., Loots, C., Antajan, E., van der Molen, J., and
1326 Travers-Trolet, M., 2015. Understanding winter distribution and trans-
1327 port pathways of the invasive ctenophore *Mnemiopsis leidyi* in the North
1328 Sea : coupling habitat and dispersal modelling approaches, *Biol. Inva-*
1329 *sions*, in press, doi :10.1007/s10530-015-0899-y.
- 1330 [23] Delpy, F., Pagano, M., Blanchot, J., Carlotti, F., & Thibault-
1331 Botha, D., 2012. Man-induced hydrological changes, metazooplank-
1332 ton communities and invasive species in the Berre Lagoon (Medi-
1333 terranean Sea, France). *Marine Pollution Bulletin*, 64(9), 1921–1932.
1334 [http ://doi.org/10.1016/j.marpolbul.2012.06.020](http://doi.org/10.1016/j.marpolbul.2012.06.020).
- 1335 [24] Donoso K., Carlotti F., Pagano M., Hunt B.P., Escribano R., Berline L.,
1336 2017. Zooplankton community response to the winter 2013 deep convec-
1337 tion proses in the NW Mediterranean Sea. *Journal of Geophysical Re-*
1338 *search : Oceans*, 122 (3), 2319-2338. ISSN 2169-9275.
- 1339 [25] Eisenhauer N., Milcu A., Nitschke N., Sabais A.C.W., Scherber C., Scheu
1340 S., 2009. Earthworm and belowground competition effects on plant pro-
1341 ductivity. *Oecologia* 161 :291–301.

- 1342 [26] Espinasse B., Carlotti F., Zhou M., Devenon J.L., 2014. Defining zoo-
1343 plankton habitats in the Gulf of Lion (NW Mediterranean Sea) using size
1344 structure and enviromental conditions. Marine Ecology progress Series,
1345 Inter-Research, 506, pp. 31-46.
- 1346 [27] Espinasse B., Basedow S., Schultes S, Zhou M., Berline L., Car-
1347 lotti F., 2017. Conditions for assessing zooplankton abundance
1348 with LOPC in coastal waters. Progress in Oceanography. *https* :
1349 *//doi.org/10.1016/j.pocean.2017.10.012*.
- 1350 [28] Finenko G.A., Abolmasova G.I. & Romanova Z.A., 1995. Consumption,
1351 respiration and growth rates of Mnemiopsis mccradyi in relation to food
1352 conditions. Biol. Morya, 21, 315–320 (in Russian).
- 1353 [29] Finenko G.A., Abolmasova G.I., Romanova Z.A., Datsyk N.A., Annins-
1354 kii B.E., 2013. Population dynamics of the ctenophore Mnemiopsis leidyi
1355 and its impact on the zooplankton in the coastal regions of the Black
1356 Sea of the Crimean coast in 2004–2008. Oceanology 53(1) :80–88.
- 1357 [30] Finenko G.A., Romanova Z.A., Abolmasova G.I., 2000. The ctenophore
1358 Beroe ovata is a new invader to the Black Sea (in Russian). Ecol Morya
1359 50 :19–22.
- 1360 [31] Finenko G.A., Kideys A.E., Anninsky B.E., Shiganova T.A., Roohi A.,
1361 Tabari M.R., Rostami H. & Bagheri S. 2006. Invasive ctenophore Mne-
1362 miopsis leidyi in the Caspian Sea : feeding, respiration, reproduction and
1363 predatory impact on the zooplankton community. Mar. Ecol. Prog. Ser.
1364 314 : 171–185.
- 1365 [32] Finenko G.A., Romanova Z.A., Abolmasova G.I., et al., 2010. Nutrition
1366 rate of Mnemiopsis leidyi in the sea and nutrition impact on zooplank-
1367 ton, Mor. Ekol. Zh., 2010, vol. 9, no. 1, pp. 73–83.
- 1368 [33] Fontana C., Grenz C., Pinazo C., Marsaleix P., Diaz F., 2009. As-
1369 similation of SeaWiFS chlorophyll data into a 3D-coupled physi-
1370 cal–biogeochemical model applied to a freshwater-influenced coastal
1371 zone. Cont Shelf Res 29(11–12) :1397–1409.
- 1372 [34] Fuentes V.L., Angel D.L., Bayha K.M., Atienza D., Edelist D., Borde-
1373 hore C., Gili J.M., Purcell J.E., 2010. Blooms of the invasive ctenophore,

- 1374 Mnemiopsis leidyi, span the Mediterranean Sea in 2009. *Hydrobiologia*
1375 645(1) : 23–37, <http://dx.doi.org/10.1007/s10750-010-0205-z>.
- 1376 [35] Ghabooli S., Shiganova T.A., Briski E., Piraino S., Fuentes V., Thibault-
1377 Botha D., Angel D.L., Cristescu M.E., Macisaac H.J., 2013. Inva-
1378 sion pathway of the Ctenophore *Mnemiopsis leidyi* in the Mediterra-
1379 nean Sea. *PLoS One*. 2013 Nov 26 ;8(11) :e81067. doi : 10.1371/jour-
1380 nal.pone.0081067.
- 1381 [36] Galil B., Kress N., Shiganova T.A., 2009. First record of *Mnemiop-*
1382 *sis leidyi* A. Agassiz, 1865 (Ctenophora; Lobata; Mnemiidae) off
1383 the Mediterranean coast of Israel. *Aquatic Invasions* 4(1) : 357-360,
1384 <http://dx.doi.org/10.3391/ai.2009.4.2.8>.
- 1385 [37] Geider R.J., MacIntyre H.L., Kana T.M., 1998. A dynamic regulatory
1386 model of phytoplankton acclimation to light, nutrients and temperature.
1387 *Limnol Oceanogr* 43 :679–694.
- 1388 [38] Gucu A.C., 2002. Can overfishing be responsible for the successful es-
1389 tablishment of *Mnemiopsis leidyi* in the Black Sea? *Estuarine, Coastal*
1390 *and Shelf Science* 54, 439-451.
- 1391 [39] Guyennon A., Baklouti M., Diaz F., Palmieri J., Beuvier J., Lebaupin-
1392 Brossier C., Arsouze T., Béranger K, Dutay J.-C., and Moutin T.,
1393 2015. New insights into the organic carbon export in the Mediter-
1394 ranean Sea from 3-D modeling. *Biogeosciences*, 12, 7025–7046, 2015,
1395 doi :10.5194/bg-12-7025-2015.
- 1396 [40] Hamer H., Malzahn A.M., Boersma M., 2011. The invasive ctenophore
1397 *Mnemiopsis leidyi* : A threat to fish recruitment in the North Sea? *Journal*
1398 *of Plankton Research* 33(1) :137-144, DOI : 10.1093/plankt/fbq100.
- 1399 [41] Isinibilir M, Tarkan AN, Kideys AE (2004) Decreased levels of the inva-
1400 sive ctenophore *Mnemiopsis* in the Marmara Sea in 2001. In : Dumont
1401 H, Shiganova TA, Niermann U (eds). *Aquatic invasions in the Black,*
1402 *Caspian, and Mediterranean Seas. The ctenophores Mnemiopsis leidyi*
1403 *and Beroe in the Ponto-Caspian and other aquatic invasions. NATO*
1404 *Science Series, IV, Earth and Environmental Sciences, Vol. 35. Kluwer*
1405 *Academic Publishers. Dordrecht, The Netherlands, pp 155–166.*

- 1406 [42] Jaspers C., Møller L.F., Kiørboe T., 2011. Salinity gradient of the Bal-
1407 tic Sea limits the reproduction and population expansion of the newly
1408 invaded comb jelly *Mnemiopsis leidyi*. PLoS ONE 6 :e24065.
- 1409 [43] Jaspers C., Moller L.F., Kiobroe T., 2015. Reproduction rates under va-
1410 riable food conditions and starvation in *Mnemiopsis leidyi* : significance
1411 for the invasion success of a ctenophore. Journal of Plankton Research,
1412 37 (5), pp. 1011-1018.
- 1413 [44] Javidpour J., Molinero J.C., Peschutter J., Sommer U., Shiganova
1414 T., 2009. Seasonal changes and population dynamics of the cte-
1415 nophore *Mnemiopsis leidyi* after its first year of invasion in the
1416 Kiel Fjord, Western Baltic Sea. Biological Invasions 11 : 873-882,
1417 <http://dx.doi.org/10.1007/s10530-008-9300-8>.
- 1418 [45] Kideys A. E. & Romanova Z., 2001. Distribution of gelatinous macrozoo-
1419 plankton in the southern Black Sea during 1996-1999. Marine Biology
1420 139(3) :535-547, DOI : 10.1007/s002270100602.
- 1421 [46] Kideys A.E., Kovalev A.V., Shulman G.E., Gordina A.D., Bingel F.,
1422 2000. A review of zooplankton investigations of the Black Sea over the
1423 last decade. J Mar Syst 24 :355–371.
- 1424 [47] Kooijman S., 2000. Energy and mass budgets in biological systems. Uni-
1425 versity Press, Cambridge
- 1426 [48] Kremer P., 1976. Population dynamics and ecological energetics of a pul-
1427 sed zooplankton predator, the ctenophore *Mnemiopsis leidyi*. In Wiley,
1428 M. L. (ed.), Estuarine Processes. Academic Press, New York 1 : 197–215.
- 1429 [49] Kremer P. & S. Nixon, 1976. Distribution and abundance of the cteno-
1430 phore *Mnemiopsis leidyi* in Narragansett Bay. Estuar. coast. mar. Sci.
1431 4 : 627–639.
- 1432 [50] Kremer, P., 1979. Predation by the ctenophore *Mnemiopsis leidyi* in
1433 Narragansett Bay, Rhode Island. Estuaries 2 : 97–105.
- 1434 [51] Kremer P., 1982. Effect of food availability on the metabolism of the
1435 ctenophore *Mnemiopsis mccradyi*. Mar. Biol., 71, 149–156.

- 1436 [52] Kremer. P. & Reeve R., 1989. Growth dynamics of a ctenophore (Mnemiopsis) in relation to variable food supply. 11. Carbon budgets and
1437 growth model. LPlank. Res. 11 :553-574.
1438
- 1439 [53] Kremer P., 1994. Patterns of abundance for Mnemiopsis in US coastal
1440 waters - a comparative overview. Ices Journal of Marine Science 51 :
1441 347–354, <http://dx.doi.org/10.1006/jmsc.1994.1036>.
- 1442 [54] Larson R.J., 1985. Trophic ecology of gelatinous predators (Cnidaria
1443 & Ctenophora) in Saanich Inlet, Vancouver Is., B.C., Canada. Ph.D.
1444 thesis, University of Victoria, Victoria.
- 1445 [55] Lucas C.H., Pitt K.A., Purcell J.E., Lebrato M., and Condon R.H., 2011.
1446 What’s in a jellyfish ? Proximate and elemental composition and biome-
1447 tric relationships for use in biogeochemical studies. Ecology 92 :1704.
- 1448 [56] Ludwig W., Bouman A.F., Dumont E., Lespinas F., 2010. Water and
1449 nutrient fluxes from major Mediterranean and Black Sea rivers : past
1450 and future trends and their implications for the basin scale budgets.
1451 GlobBiogeochem Cycles 24 :GB0A13. doi :10.1029/2009GB003594.
- 1452 [57] Madsen C.V. & Riisgard H.U., 2010. Ingestion-rate method for measu-
1453 rement of clearance rates of the ctenophore Mnemiopsis leidyi. Aquatic
1454 Invasions. 2010. V. 5. P. 357–361.
- 1455 [58] Mills C.E., 2001. Jellyfish blooms : are populations increasing globally
1456 in response to changing ocean conditions ? Hydrobiologia, 451, 55–68.
- 1457 [59] Miller R. J., 1974. Distribution and Biomass of an Estuarine Ctenophore
1458 Population, Mnemiopsis leidyi (A. Agassiz). Chesapeake Science, 15 :1-
1459 8.
- 1460 [60] Nowaczyk A., Carlotti F., Thibault Botha D., Pagano M., 2011. Dis-
1461 tribution of epipelagic metazooplankton across the Mediterranean Sea
1462 during the summer BOUM cruise. Biogeosciences, 8 (8), 2159-2177, ISSN
1463 1726-4170.
- 1464 [61] Oguz, T., B. Fach & B. Salihoglu, 2008. Invasion dynamics of the alien
1465 ctenophore Mnemiopsis leidyi and its impact on anchovy collapse in the
1466 Black Sea. Journal of Plankton Research 30 : 1385–1397.

- 1467 [62] Pitois S. & Shiganova T., CIESM, 2015. Report of the Joint
 1468 CIESM/ICES Workshop on Mnemiopsis Science [co-edited by S.Pitois
 1469 and T.Shiganova] 18-20 september 2014, Coruna, Spain. 3.4, pp.18-21 /
 1470 ICES. 2014. Report of the Joint CIESM/ICES Workshop on Mnemiopsis
 1471 Science (JWMS), 18–20 September 2014, A Coruña, Spain. ICES CM
 1472 2014/SSGHIE :14. pp.18-21.
- 1473 [63] Pitt K.A. & Lucas C.H., 2013. Jellyfish Blooms. ISBN 978-94-007-7015-
 1474 7.
- 1475 [64] Purcell J.E., D. A. Nemazie, S.E.Dorsey, E.D.Houde, & J. C. Gamble.
 1476 1994. Predation mortality of bay anchovy eggs and larvae due to scy-
 1477 phomedusae and ctenophores in Chesapeake Bay. Mar. Ecol. Prog. Ser.
 1478 114 : 47–58, doi :10.3354/meps114047.
- 1479 [65] Purcell J.E., Shiganova T.A., Decker M.B. and Houde E.D., 2001.
 1480 The ctenophore Mnemiopsis in native and exotic habitats : U.S. es-
 1481 tuaries versus the Black Sea basin. Hydrobiologia 451 : 145-176,
 1482 <http://dx.doi.org/10.1023/A:1011826618539>.
- 1483 [66] Rapoza R., Novak D., and Costello J. H., 2005. Life-stage dependent, in
 1484 situ dietary patterns of the lobate ctenophore Mnemiopsis leidyi Agassiz
 1485 1865. Journal of Plankton Research, 27(9) :951–956.
- 1486 [67] Reeve M.R., Syms M.A., Kremer P., 1989. Growth dynamics of a cteno-
 1487 phore (Mnemiopsis) in relation to variable food supply. I. Carbon bio-
 1488 mass, feeding, egg production, growth and assimilation efficiency. Jour-
 1489 nal of Plankton Research 11, 535–552.
- 1490 [68] Salihoglu B., Fach B.A., Oguz T., 2011. Journal of Marine Systems,
 1491 87(1), 55-65.
- 1492 [69] Salihoglu B., Sevinc N., 2013. Quantification of the Synergistic Effects of
 1493 Eutrophication, Apex Predator Pressure, and Internal Processes on the
 1494 Black Sea Ecosystem. Turkish Journal of Fisheries and Aquatic Sciences
 1495 13 : 581-592, DOI :10.4194/1303-2712-v13_4_03.
- 1496 [70] Sasson D.A., Ryan J.F., 2016. The sex lives of ctenophores : the influence
 1497 of light, body size, and self-fertilization on the reproductive output of the
 1498 sea walnut, Mnemiopsis leidyi. PeerJ 4 :e1846 ; DOI 10.7717/peerj.1846.

- 1499 [71] Shiganova T.A. & Bulgakova Y.V., 2000. Effect of gelatinous plankton
1500 on the Black and Azov Sea fish and their food resources. ICES J Mar
1501 Sci 57 :641-648.
- 1502 [72] Shiganova, T.A., Bulgakova, Y.V., Volovik, S.P., Mirzoyan, Z.A., Dud-
1503 kin, S.I., 2001a. A new invader, *Beroe ovata* Mayer 1912 and its effect on
1504 the ecosystems of the Black and Azov Seas. In : In : Purcel, J.E., Gra-
1505 ham, W.M., Dumont, H.J. (Eds.), *Hydrobiologia* 451, vol. 451. Kluwer
1506 Ac.pub, pp. 187–197.
- 1507 [73] Shiganova T., Mirzoyan Z., Studenikina E., Volovik S., Siokou-Frangou
1508 I., Zervoudaki S., Christou E., Skirta A., Dumont H., 2001b. Popula-
1509 tion development of the invader ctenophore *Mnemiopsis leidyi* in the
1510 Black Sea and other seas of the Mediterranean basin. *Journal of Marine*
1511 *Biology* 139 : 431–445, doi :10.1007/s002270100554.
- 1512 [74] Shiganova T., Alekseenko E., Moskalenko L., Nival P., 2018. Modelling
1513 assessment of interactions in the Black Sea of the invasive ctenophores
1514 *Mnemiopsis leidyi* and *Beroe ovata*. *Ecological Modelling*, 376 (2018)
1515 1-14. DOI :10.1016/j.ecolmodel.2018.02.008.
- 1516 [75] Siapatis, A., M. Giannoulaki, V. D. Valavanis, A. Pali Alexis, E. Schis-
1517 menou, A. Machias & S. Somarakis, 2008. Modeling potential habitat of
1518 the invasive ctenophore *Mnemiopsis leidyi* in Aegean Sea. *Hydrobiologia*
1519 612 : 281–295.
- 1520 [76] Stoecker D.K., Verity P.G., Michaels A.E. et al., 1987. Feeding by larval
1521 and post-larval ctenophores on microzooplankton. *J. Plankton Res.*, 9,
1522 667–683.
- 1523 [77] Sullivan L.J. & Gifford D.J., 2004. Diet of the larval ctenophore *Mne-*
1524 *miopsis leidyi* A. Agassiz (Ctenophora, Lobata). *Journal of Plankton*
1525 *Research* , 26, 417-431.
- 1526 [78] Sullivan L.J. & Gifford D.J., 2007. Growth and feeding rates of the newly
1527 hatched larval ctenophore *Mnemiopsis leidyi* A. Agassiz (Ctenophora,
1528 Lobata). *Journal of Plankton Research* , 29, 949-965.
- 1529 [79] The MerMex Group : Durrieu deMadron X., Guieu C., Sempéré R., Co-
1530 nan P., Cossa D., D’Ortenzio F., Estournel C., Gazeau F., Rabouille C.,

- 1531 Stemmann L., Bonnet S., Diaz F., Koubbi P., Radakovitch O., Babin
1532 M., Baklouti M., Bancon-Montigny C., Belviso S., Bensoussan N., Bon-
1533 sang B., Bouloubassi I., Brunet C., Cadiou J.-F., Carlotti F., Chami
1534 M., Charmasson S., Charrière B., Dachs J., Doxaran D., Dutay J.-C.,
1535 Elbaz-Poulichet F., Eléaume M., Eyrolles F., Fernandez C., Fowler S.,
1536 Francour P., Gaertner J.C., Galzin R., Gasparini S., Ghiglione J.-F.,
1537 Gonzalez J.-L., Goyet C., Guidi L., Guizien K., Heimbürger L.-E., Jac-
1538 quet S.H.M., Jeffrey W.H., Joux F., Le Hir P., Leblanc K., Lefèvre D.,
1539 Lejeusne C., Lemé R., Loÿe-Pilot M.-D., Mallet M., Méjanelle L., Mélin
1540 F., Mellon C., Mérigot B., Merle P.-L., Migon C., Miller W.L., Mortier
1541 L., Mostajir B., Mousseau L., Moutin T., Para J., Pérez T., Petrenko
1542 A., Poggiale J.-C., Prieur L., Pujo-Pay M., Pulido-Villena E., Raim-
1543 bult P., Rees A.P., Ridame C., Rontani J.-F., Ruiz Pino D., Sicre M.A.,
1544 Taillandier V., Tamburini C., Tanaka T., Taupier-Letage I., Tedetti M.,
1545 Testor P., Thébault H., Thouvenin B., Touratier F., Tronczynski J.,
1546 Ulses C., Van Wambeke F., Vantrepotte V., Vaz S., Verney R., 2011.
1547 Marine ecosystems' responses to climatic and anthropogenic forcings in
1548 the Mediterranean. *Prog Oceanogr* 91 :97–166.
- 1549 [80] van der Molen J., van Beek J., Augustine S., Vansteenbrugge L., van
1550 Walraven L., Langenberg V., van der Veer H. W., Hostens K., Pitois
1551 S., and Robbens J., 2015. Modelling survival and connectivity of *Mne-*
1552 *miopsis leidyi* in the southern North Sea and Scheldt estuaries. *Ocean*
1553 *Sci. Discuss.*, 10, 1–51, 2014, doi :10.5194/osd-10-1-2014.
- 1554 [81] Vilà M., Basnou C., Pyšek P., Josefsson M., Genovesi P., Gollasch S.,
1555 Nentwig W., Olenin S., Roques A., Roy D., Hulme P. and DAISIE part-
1556 ners, 2010. 'How well do we understand the impacts of alien species on
1557 ecosystem services? A pan European cross-taxa assessment', *Frontiers*
1558 *of Ecology and Environment*, (8) 135–144.
- 1559 [82] Waggett R. & Costello J. H., 1999. Capture mechanisms used by the
1560 lobate ctenophore, *Mnemiopsis leidyi*, preying on the copepod *Acartia*
1561 *tonsa*. *J. Plankton Res.* 21 :2037–2052, doi :10.1093/plankt/21.11.2037.
- 1562 [83] Weber T. & Deutsch C., 2012. Oceanic nitrogen reservoir regulated
1563 by plankton diversity and ocean circulation. *Nature* 489, 419–422,
1564 doi :10.1038/nature11357.

1565 [84] Werschkun B., Banerji S., Basurko O.C., David M., Fuhr F., Gollasch
1566 S., Grummt T., Haarich M., Jha A.N., Kacan S., Kehrer A., Linders J.,
1567 Mesbahi E., Pughiucm D., Richardson S.D., Schwarz-Schulz B., Shah
1568 A., Theobald N., von Gunten U., Wieck S., & Höfer T., 2014. Emerging
1569 risks from ballast water treatment : The run-up to the International
1570 Ballast Water Management Convention. *Chemosphere*, 112, 256-266.

FIGURES and TABLES

FIGURE 1: Reports of ML blooms in the Mediterranean Sea from Fuentes et al. (2010) - black symbols - and Kylie and Lucas (2014) and Boero (2009) - red symbols.

TABLE 1: Model symbols and parameters for ML. Parameter values have been taken or estimated from measured data from Salihouglu et al., 2011[1],2013[2]; Kylie et al., 2009[3], Madsen & Riisgard, 2010[4]; Lucas et al., 2011[5]

Symbol	Definition	Units	Value	Reference
ML	ML abundance	$ind.l^{-1}$		
<i>Intracellular contents and growth</i>				
Q_{10}	Q10-temperature coefficient	-	1.5	[2]
$\bar{\mu}$	maximum specific growth rate	s^{-1}	$4.62 \cdot 10^{-6}$	[2]
σ	proportion of the minimum internal quota in immature adult (see Section 3.2)	-	0.85	
Q_C^{max}	maximum carbon content	$mol.ind^{-1}$	$2.58 \cdot 10^{-4}$	[1]
Q_C^{min}	minimum carbon content	$mol.ind^{-1}$	$Q_C^{max}/3$	
Q_C^{mean}	mean carbon content	$mol.ind^{-1}$	$2Q_C^{min}$	
Q_N^{mean}	mean nitrogen content	$mol.ind^{-1}$	Q_C^{mean}/Q_{CN}^{mean}	
Q_N^{min}	minimum nitrogen content	$mol.ind^{-1}$	$Q_N^{mean}/2$	
Q_N^{max}	maximum nitrogen content	$mol.ind^{-1}$	$3Q_N^{min}$	
Q_P^{mean}	mean phosphate content	$mol.ind^{-1}$	Q_C^{mean}/Q_{CP}^{mean}	
Q_P^{min}	minimum phosphate content	$mol.ind^{-1}$	$Q_P^{mean}/2$	
Q_P^{max}	maximum phosphate content	$mol.ind^{-1}$	$3Q_P^{min}$	
Q_{CN}^{mean}	mean C:N ratio in ML.	$mol.mol^{-1}$	4.13	[3,5]
Q_{CN}^{min}	minimum C:N ratio in ML.	$mol.mol^{-1}$	Q_C^{min}/Q_N^{max}	
Q_{CN}^{max}	maximum C:N ratio in ML.	$mol.mol^{-1}$	Q_C^{max}/Q_N^{min}	
Q_{CP}^{mean}	mean C:P ratio in ML.	$mol.mol^{-1}$	99.8	
Q_{CP}^{min}	minimum C:P ratio in ML.	$mol.mol^{-1}$	Q_C^{min}/Q_P^{max}	
Q_{CP}^{max}	maximum C:P ratio in ML.	$mol.mol^{-1}$	Q_C^{max}/Q_P^{min}	
<i>Feeding</i>				
F	clearance rate (prey1)	$l \text{ ind}^{-1} s^{-1}$	$5.28 \cdot 10^{-5}$	[4]
I_{MAX}	max. ingestion rate (prey1)	$ind \text{ ind}^{-1} s^{-1}$	0.00103	[4]
α_1	proportion of Z ingested by ML juveniles		0.8	
α_2	proportion of CIL ingested by ML juveniles		0.2	
<i>Mortality</i>				
k_m	specific natural mortality rate	s^{-1}	$5.787 \cdot 10^{-8}$	[2]
A	constant in mortality function	s^{-1}	$3.87 \cdot 10^{-10}$	
k_{mq}	specific quadratic mortality rate	$l.ind^{-1}.s^{-1}$	10^{-7}	
<i>Respiration and excretion</i>				
r_m	respiration-excretion rate	s^{-1}	$2.89 \cdot 10^{-7}$	
r_i	respiration rate for ingestion demands	-	0.2	

TABLE 2: List of functions used to describe ML physiology in the model.

Symbol	Definition	Unit
f^μ	Specific growth rate	s^{-1}
f_{ML}^{gz}	Specific feeding rate of z by ML	s^{-1}
f_{gjuv}	Specific feeding rate during juvenile stages	s^{-1}
f^m	Specific natural mortality rate	s^{-1}
f^{mq}	Specific quadratic mortality rate (implicit feeding)	$l.ind^{-1}.s^{-1}$
f^{resp}	Specific respiration rate	s^{-1}
f_{excr}^X	Specific excretion rate	s^{-1}
h_{QX}	Quota function for element X among C, N and P	-

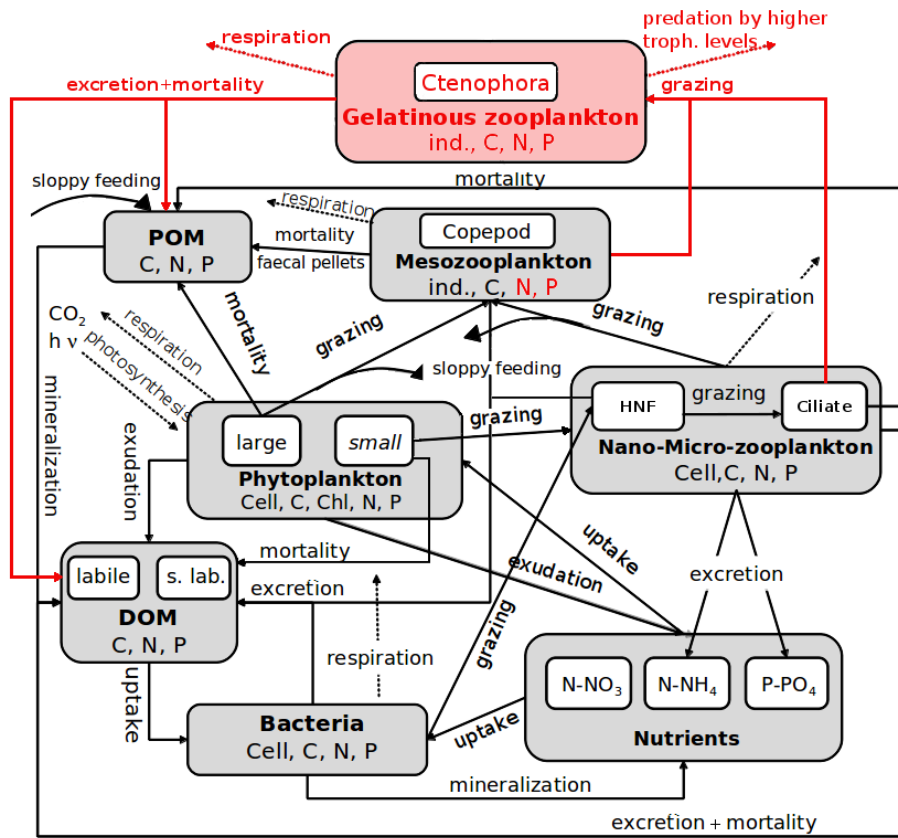


FIGURE 2: In grey – conceptual scheme of the biogeochemical model for the NW Mediterranean Sea (Eco3M-MED, Alekseenko et al. 2014) implemented in the Eco3M tool; in red - additional variables and processes : namely one functional group of carnivorous gelatinous plankton and associated processes, and two new variables expressing N and P contents in mesozooplankton.

TABLE 3: Forcings taken into account in the modelling scenarios. *calc - means dynamically calculated by the biogeochemical model including the low trophic levels.

Scenario	day/night light variation	seasonal light variation	seasonal temperature variation	copepod abundance	batch (B)- chemostat (C)
<i>TS1</i>	YES	NO	NO	fixed	B
<i>TS2</i>	YES	NO	NO	fixed	B
<i>TS3</i>	YES	NO	NO	fixed	B
<i>TS4</i>	YES	YES	YES	*calc	B
<i>TS5</i>	YES	YES	YES	calc	C
<i>TS6</i>	YES	YES	YES	calc	B

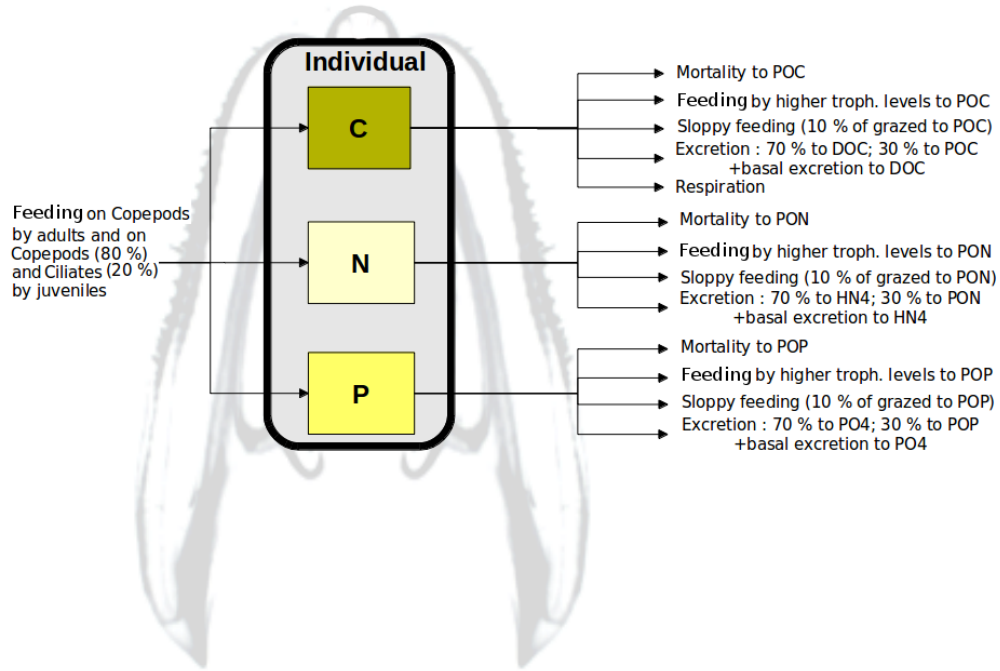


FIGURE 3: Physiological processes undertaken by ML and taken into account in the model.

TABLE 4: Test series TS2a. Synthesis of simulated experiments with final values of three indicators : t_{rep} , Fl_Q and SPGR. t_{rep} : time necessary to reach the adult stage mature for reproduction ; Fl_Q : mean ML carbon accumulation rate over t_{rep} ; SPGR : specific population growth rate (in h^{-1}) between the 8th and the 12th week depending on the available copepod abundance (Z in $ind.l^{-1}$) of 2.5, 5, 10, 25, 100 and 250 $ind.l^{-1}$ with copepod \widetilde{Q}_C equal to 50% and $\widetilde{Q}_N = \widetilde{Q}_P = 100\%$.

Copepod abundance (Z) with $\widetilde{Q}_C = 50\%$ ($ind.l^{-1}$)	Copepod Carbon biomass ($molC.l^{-1}$)	t_{rep} (h)	Fl_Q ($molC.ind^{-1}.h^{-1}$)	$SPGR$ (h^{-1})
2.5	$1.25 \cdot 10^{-6}$	-	-	$-4.77 \cdot 10^{-4}$
5	$2.5 \cdot 10^{-6}$	129	$1 \cdot 10^{-7}$	0.0022
10	$5 \cdot 10^{-6}$	47	$2.75 \cdot 10^{-7}$	0.0105
25	$1.25 \cdot 10^{-5}$	23	$5.61 \cdot 10^{-7}$	0.0505
100	$5 \cdot 10^{-5}$	14.4	$8.96 \cdot 10^{-7}$	0.1431
250	$1.25 \cdot 10^{-4}$	12.2	$1.06 \cdot 10^{-6}$	0.1830

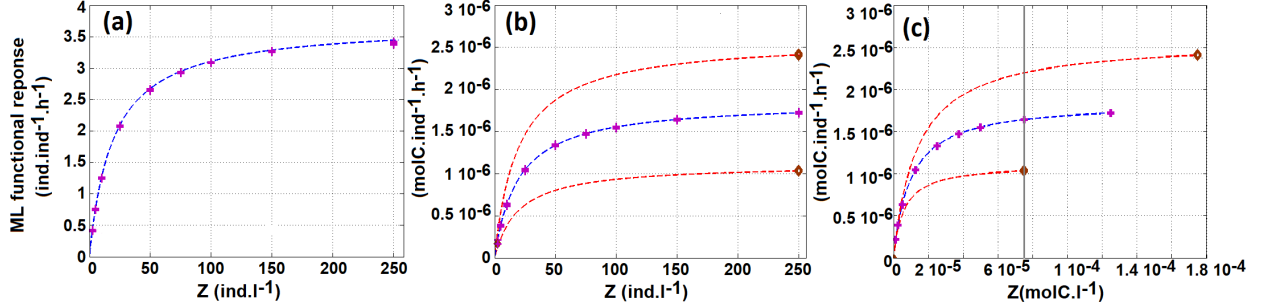


FIGURE 4: Test series TS1. Functional response for ML depending on the prey (i.e. copepod, Z) abundance and biomass. (a) Magenta crosses : values of simulated ingestion rate (in $\text{ind}\cdot\text{ind}^{-1}\cdot\text{h}^{-1}$) at steady state for the 9 food level experiments (in $\text{ind}\cdot\text{l}^{-1}$) for copepods with \widetilde{Q}_C equal to 50%. Dotted blue line corresponds to the theoretical functional response for ML predation (Eq.2), (b and c) Magenta crosses : values of ingestion rate (in $\text{molC}\cdot\text{ind}^{-1}\cdot\text{h}^{-1}$) at steady state for the 9 food level experiments (in $\text{ind}\cdot\text{l}^{-1}$) for copepod with \widetilde{Q}_C equals to 50%. Brawn diamonds : values of ingestion rate (in $\text{molC}\cdot\text{ind}^{-1}\cdot\text{h}^{-1}$) at steady state for the highest food level experiment (in $\text{ind}\cdot\text{l}^{-1}$) for copepod with \widetilde{Q}_C equals to 0 and 100% (respectively lower and upper diamonds). Dotted lines : theoretical functional responses expressed in $\text{molC}\cdot\text{ind}^{-1}\cdot\text{h}^{-1}$ for different copepod \widetilde{Q}_C values. Dotted blue line : same as in (a) with copepod \widetilde{Q}_C equal to 50%. but with ingestion rate expressed in $\text{molC}\cdot\text{ind}^{-1}\cdot\text{h}^{-1}$. Dotted red lines : with copepod \widetilde{Q}_C equal to 0% (lower dotted red line) and to 100% (upper dotted red line). Grey vertical line represent three values of copepod abundance with three different internal Quotas of Carbon chosen in the TS2b test series.

TABLE 5: Test series TS3. Time delays between the recovery of ML individual feeding activity and the restart of ML population growth (t_2-t_1) for the starvation/replenishment tests with food abundance at $10 \text{ ind}\cdot\text{l}^{-1}$ and $5 \text{ ind}\cdot\text{l}^{-1}$ presented in Fig.7.

Feeding start t_1 (weeks)	$t_2 - t_1$ (days) for two copepod levels	
	$Z=5 \text{ ind}\cdot\text{l}^{-1}$	$Z=10 \text{ ind}\cdot\text{l}^{-1}$
4	17.8	6.5
6	19.3	8.6
8	21.1	9.3
12	22.5	10.5

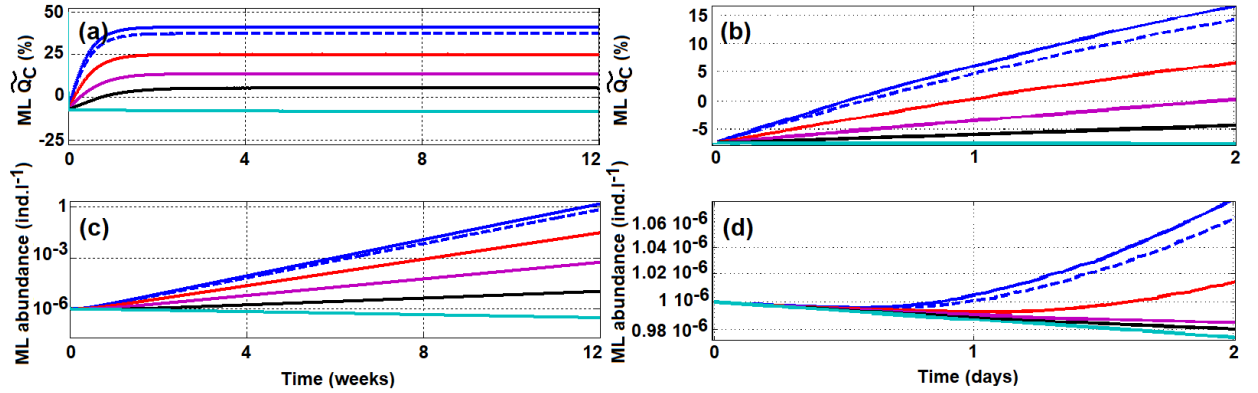


FIGURE 5: Test series TS2a. Temporal dynamics of ML individual carbon relative \widetilde{Q}_C (a and b) and ML population abundance (c and d) for different constant food levels. Simulation over 12 weeks (a and c) and zoom during the two first days (b and d). ML population starts with $1 \cdot 10^{-6} \text{ ind.l}^{-1}$ and with individual quotas $\widetilde{Q}_C = 50\%$ and $\widetilde{Q}_N = \widetilde{Q}_P = 100\%$; Levels of food abundances (Z): 2.5 (light blue line), 5 (black line), 10 (magenta line), 25 (red line), 100 (blue dotted line) and 250 (blue line) ind.l^{-1} , with copepod \widetilde{Q}_C equal to 50% and $\widetilde{Q}_N = \widetilde{Q}_P = 100\%$. $T=15^\circ\text{C}$.

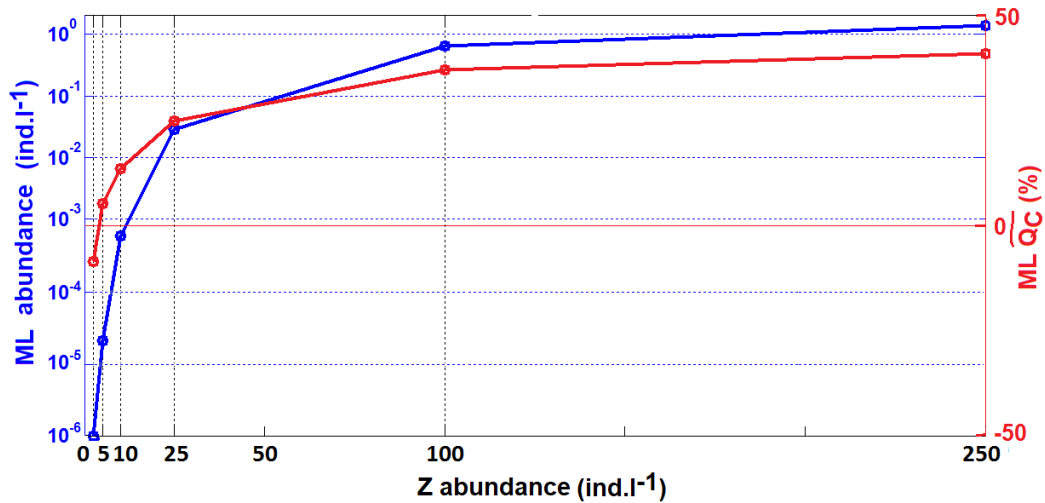


FIGURE 6: Test series TS2a. Synthesis of simulated experiments in constant food conditions: ML abundance (ind.l^{-1}) and $\widetilde{Q}_C(\%)$ 12 weeks after the start of simulation depending on the available copepod abundance (Z in ind.l^{-1}) of 2.5, 5, 10, 25, 100 and 250 ind.l^{-1} with copepod \widetilde{Q}_C equal to 50% and $\widetilde{Q}_N = \widetilde{Q}_P = 100\%$; $T=15^\circ\text{C}$.

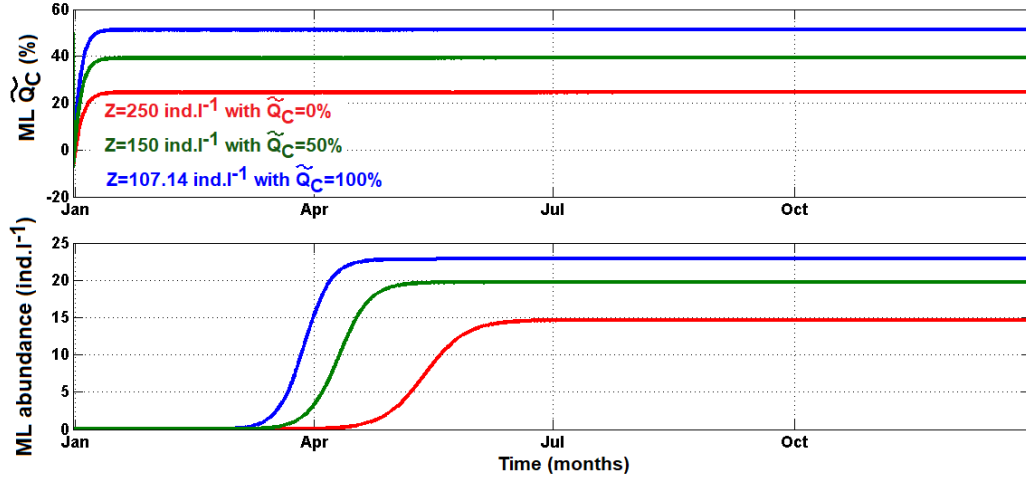


FIGURE 7: Test series TS2b. Temporal dynamics of ML individual carbon relative \widetilde{Q}_C and ML population abundance for constant copepod Carbon biomass conditions of $7.5 \cdot 10^{-5} \text{ molC.l}^{-1}$ depending on the available copepod quantity and quality (ind.l^{-1}) of 250 ind.l^{-1} with $\widetilde{Q}_C=0\%$ (red line), 150 ind.l^{-1} with $\widetilde{Q}_C=50\%$ (green line), and $107.14 \text{ ind.l}^{-1}$ with $\widetilde{Q}_C=100\%$ (blue line). For ML and copepods we consider $\widetilde{Q}_N=\widetilde{Q}_P = 100\%$; $T=15^\circ$.

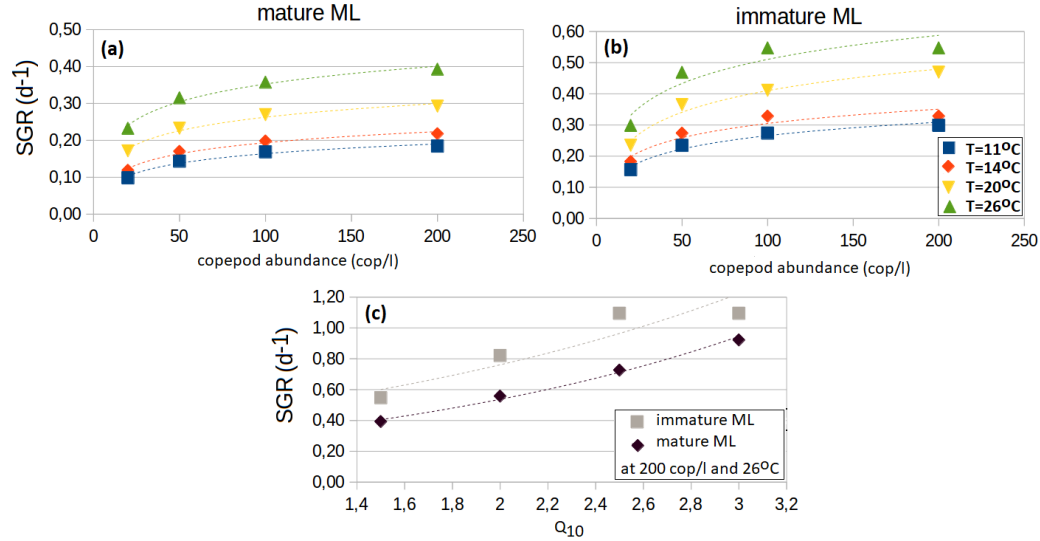


FIGURE 8: Test series TS2c. Estimation of SGR (d^{-1}) values for mature ML (a) and immature ML (b) depending on the constant copepod abundance in different temperature conditions, at $Q_{10} = 1.5$; (c) SGR values for mature and immature ML at constant copepod abundance of 200 ind.l^{-1} with $\widetilde{Q}_C=100\%$ and at the temperature of 26°C depending on the choice of Q_{10} . Dotted lines show estimated trends for each experiment.

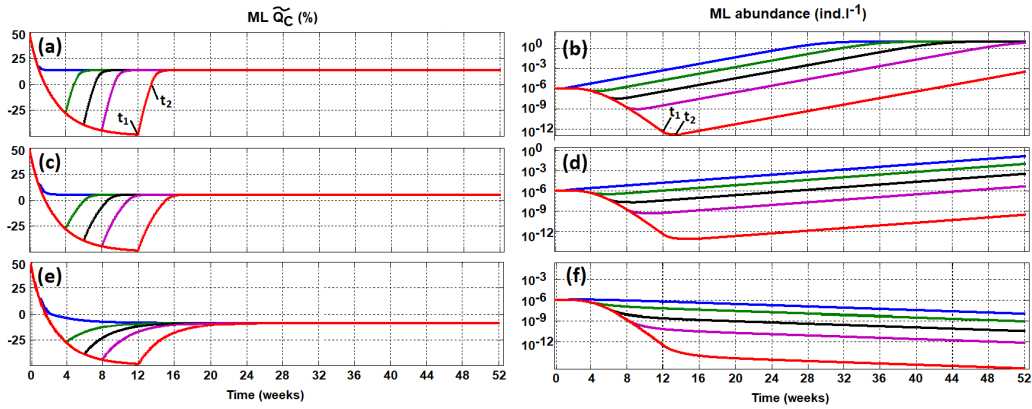


FIGURE 9: Test series TS3. Tests on starvation durations followed by food recovery at different food levels. Temporal dynamics of ML individual carbon relative \widetilde{Q}_C (left column) and ML population abundance (right column) for different food replenishment levels (a and b : $Z=10 \text{ ind.l}^{-1}$, c and d : $Z=5 \text{ ind.l}^{-1}$, e and f : $Z=2.5 \text{ ind.l}^{-1}$) and for different starvation durations (blue line : 1 week, green line : 4 weeks, black line : 6 weeks, magenta line : 8 weeks and red line : 12 weeks). Copepod \widetilde{Q}_C equal to 50% and $\widetilde{Q}_N = \widetilde{Q}_P = 100\%$. $T=15^\circ\text{C}$. As an example, for the 12 weeks starvation experiment : t_1 corresponds to the starting date of food recovering and ML individual growth recovery and t_2 - to the ML reproduction starting date ($\widetilde{Q}_C=0\%$).

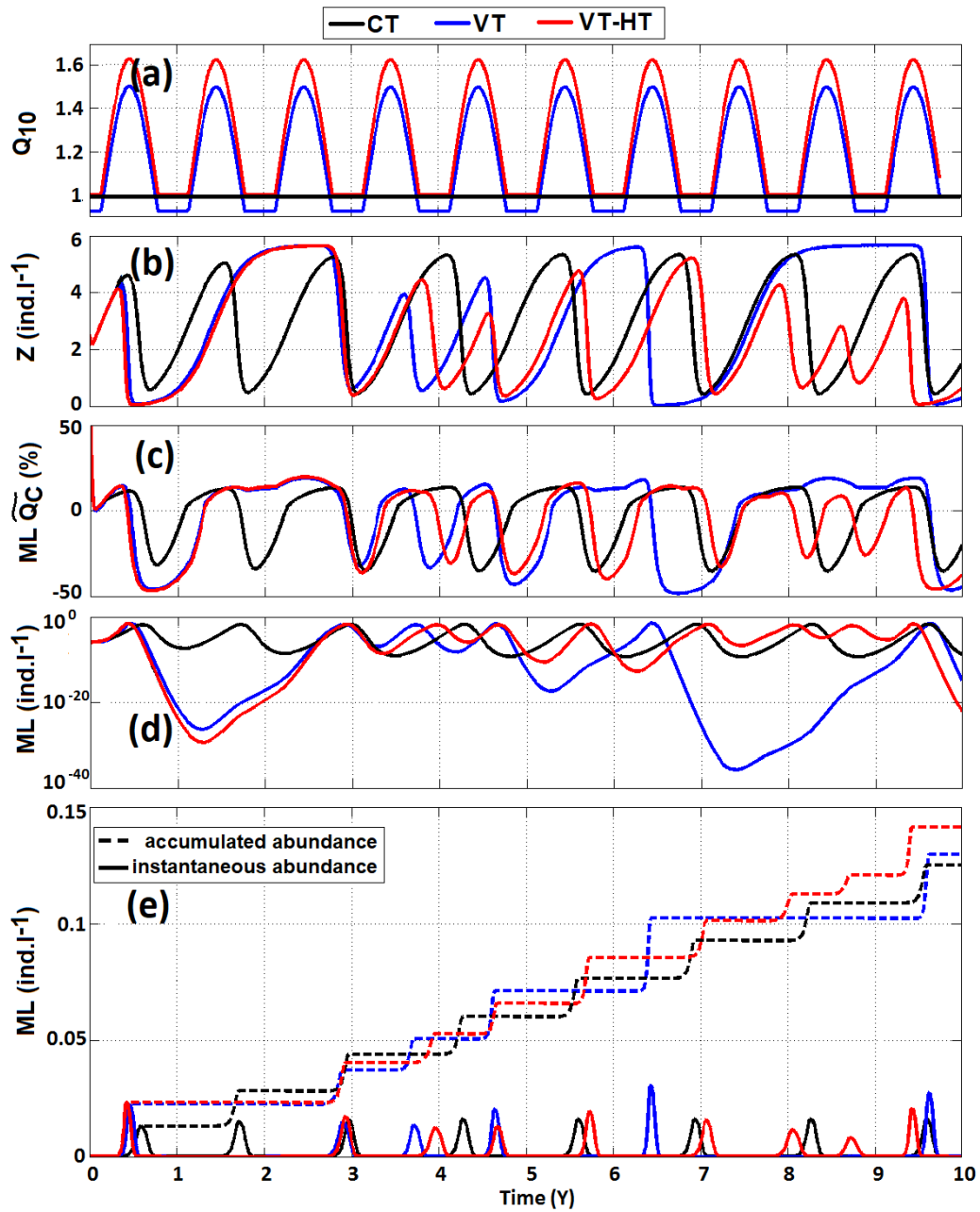


FIGURE 10: Test series TS4. Temperature impact on : a) Q_{10} variaion, b) copepod abundance (Z in ind.l⁻¹), c) ML relative quota of carbon (%, d) ML abundance (ind.l⁻¹) in log scale and e) ML abundance : instantaneous and accumulated values (ind.l⁻¹). Black line - no temperature taken into account (CT case), blue line - T_{ref} temperature taken into account in the physiology of ML (VT case), red line - $T_{ref} + 2^{\circ}C$ temperature taken into account in the physiology of ML (VT-HT case).

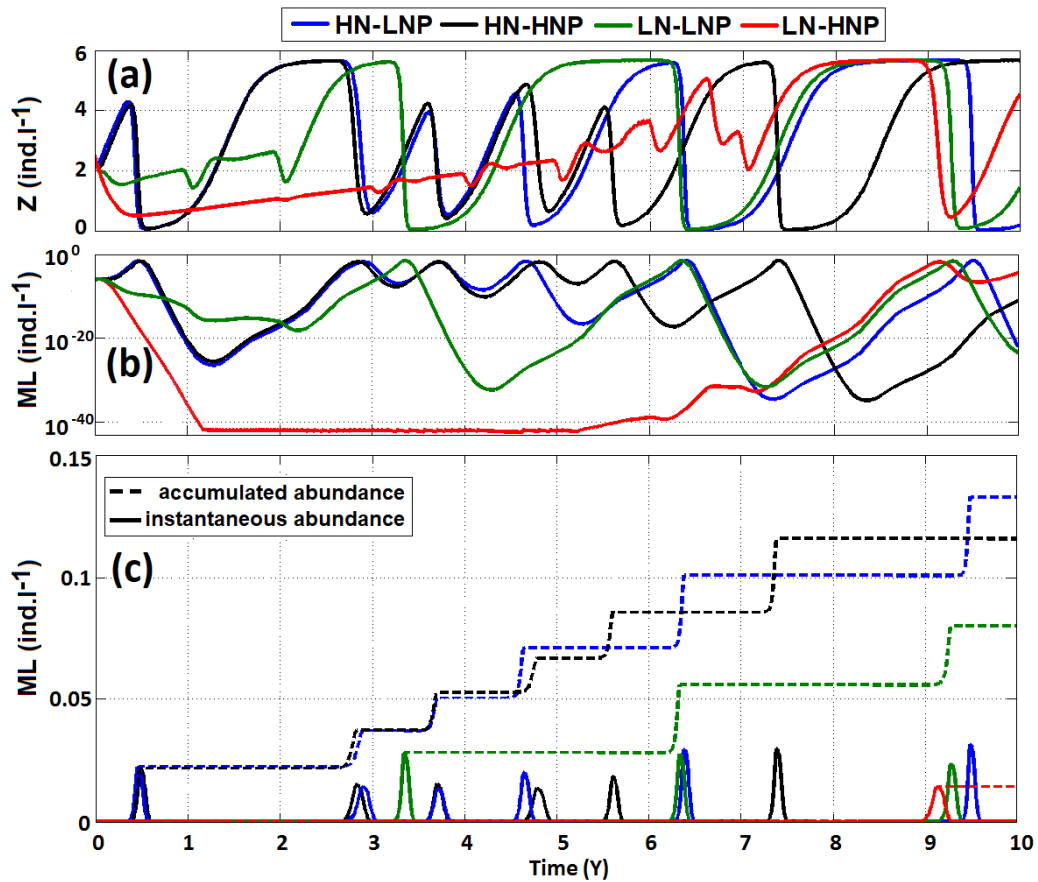


FIGURE 11: Test series TS5. Nutrient ratio impact on a) copepod abundance (Z in ind.l⁻¹), b) ML abundance in log scale in ind.l⁻¹ and c) ML abundance : instantaneous and accumulated values (ind.l⁻¹). Blue line - $NO_3=5 \mu M$ and $NO_3 : PO_4=20$ (HN-LNP case), black line - $NO_3=5 \mu M$ and $NO_3 : PO_4=40$ (HN-HNP case), green line - $NO_3=1.25 \mu M$ and $NO_3 : PO_4=20$ (LN-LNP case), red line - $NO_3=1.25 \mu M$ and $NO_3 : PO_4=40$ (LN-HNP case).

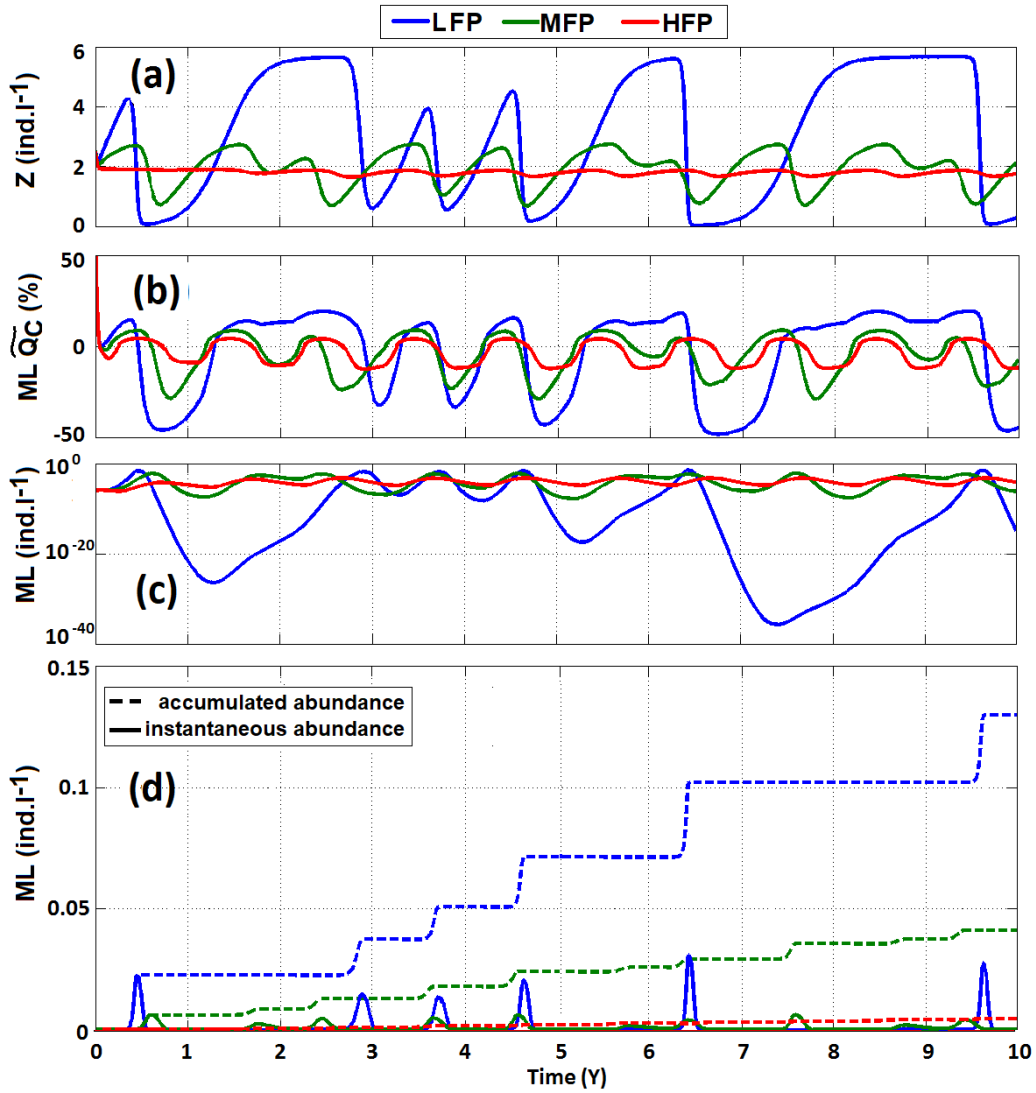


FIGURE 12: Test series TS6. Impact of competitive pressure on ML prey : a) copepod abundance (Z in ind.l⁻¹), b) ML relative quota of carbon (%) and c) ML abundance in log scale in ind.l⁻¹ and d) ML abundance : instantaneous and accumulated values (ind.l⁻¹). Blue line - reference test with $f_Z^{mq} = \lambda s^{-1}$ (LFP case), green line - $f_Z^{mq} = 2\lambda s^{-1}$ (MFP case), red line - $f_Z^{mq} = 3\lambda s^{-1}$, where $\lambda = 3 \cdot 10^{-8} s^{-1}$ (HFP case).